Sedimentology (2004) **51,** 1–27 doi: 10.1111/j.1365-3091.2004.00670.x

Implications for Neoarchaean ocean chemistry from primary carbonate mineralogy of the Campbellrand-Malmani Platform, South Africa

DAWN Y. SUMNER* and JOHN P. GROTZINGER†
**Department of Geology, University of California, Davis, CA 95616, USA*
(E-mail: sumner@geology.ucdavis.edu)
†Earth, Atmospheric and Planetary Sciences, Massachusetts Institute of Technology, Cambridge, MA, USA

ABSTRACT

The precipitation of calcite and aragonite as encrustations directly on the seafloor was an important platform-building process during deposition of the 2560–2520 Ma Campbellrand-Malmani carbonate platform, South Africa. Aragonite fans and fibrous coatings are common in unrestricted, shallow subtidal to intertidal facies. They are also present in restricted facies, but are absent from deep subtidal facies. Decimetre-thick fibrous calcite encrustations are present to abundant in all depositional environments except the deepest slope and basinal facies. The proportion of the rock composed of carbonate that precipitated as encrustations or in primary voids ranges from 0% to > 65% depending on the facies. Subtidal facies commonly contain 20–35% *in situ* precipitated carbonate, demonstrating that Neoarchaean sea water was supersaturated with respect to aragonite, carbonate crystal growth rates were rapid compared with sediment influx rates, and the dynamics of carbonate precipitation were different from those in younger carbonate platforms. The abundance of aragonite pseudomorphs suggests that sea-water pH was neutral to alkaline, whereas the paucity of micrite suggests the presence of inhibitors to calcite and aragonite nucleation in the mixed zone of the oceans.

Keywords Aragonite, atmospheric carbon dioxide, calcite, carbonate saturation state, microbialites, siderite, stromatolites.

INTRODUCTION

Carbonate rocks reflect the biological and geochemical evolution of the oceans and are a rich source of information on early Earth ocean chemistry and the early evolution of life. Carbonate textures have been used to interpret large geochemical changes in early Earth history as well as the smaller changes that occurred during Phanerozoic time (e.g. Sandberg, 1985; Wilkinson & Given, 1986; Grotzinger, 1989; Opdyke & Wilkinson, 1993; Grotzinger & Knoll, 1995; Hardie, 1996; Kah & Knoll, 1996). Changes in ocean chemistry such as a significant increase in oxidation state at about 2·2 Ga and a long-term decline in atmospheric CO_2 probably had a substantial influence on the chemistry and texture of Proterozoic and Archaean carbonates (Grotzinger, 1990; Grotzinger & Kasting, 1993; Kah & Knoll, 1996; Sumner & Grotzinger, 1996a; Sumner, 2001; Bekker & Eriksson, 2003), although reliable models for the specific influences of these changes have yet to be developed and tested. The first step in developing such models is to document temporal changes in carbonate facies, which can then be correlated to other indicators of changes in geochemical cycles. For example, Neoarchaean carbonates commonly contain centimetre- to metre-thick beds of aragonite and calcite crystals that grew directly on the seafloor from open-marine waters (Hofmann, 1971; Simonson *et al.*, 1993; Kusky & Hudleston,

1999; Sumner & Grotzinger, 2000; Sumner, 2001; Hofmann *et al.*, 2004). Encrustations such as these are rare to absent in most Proterozoic and Phanerozoic open-marine carbonates, although exceptions are present (e.g. Grotzinger & Knoll, 1995; Grotzinger & Rothman, 1996; Kah & Knoll, 1996; James *et al.*, 2001; Sumner, 2001; Nogueira *et al.*, 2003). Characterizing the depositional patterns of *in situ* calcite and aragonite precipitation is likely to lead to constraints on Neoarchaean ocean chemistry and the long-term evolution of Earth's biogeochemical cycles.

Most Neoarchaean carbonates are preserved as relatively thin build-ups covering areas of less than a few hundred square kilometres (see review by Grotzinger, 1989; and Hofmann *et al.*, 1985; Wilks, 1986; Hofmann & Masson, 1994). Typically, several facies representing closely related depositional environments are preserved in any given occurrence, limiting the potential for the development of regional stratigraphic constraints on depositional environments and for detailed studies of lateral facies transitions. The roughly correlative Wittenoom Formation and Carawine Dolomite, Hamersley Basin, Australia (Simonson *et al.*, 1993), and the Campbellrand-Malmani carbonate platform, Transvaal Supergroup, South Africa (e.g. Button, 1973; Eriksson & Truswell, 1974; Beukes, 1987), are two examples of well-preserved Neoarchaean carbonate platforms with broader facies distributions. The Campbellrand-Malmani platform, in particular, contains preserved depositional environments ranging from deep subtidal to supratidal that can be correlated over 800 km across strike. This extensively preserved platform provides the opportunity to constrain depositional environments and facies transitions across an entire Neoarchaean carbonate platform. In addition, petrographic textures are exceedingly well preserved, allowing documentation of the styles and abundance of *in situ* precipitation of calcite and aragonite crystals directly on the seafloor. Thus, the Campbellrand-Malmani platform provides a fantastic opportunity to establish constraints on the dynamics of Neoarchaean carbonate precipitation.

GEOLOGICAL BACKGROUND

The 2588–2520 Ma (Barton *et al.*, 1994; Walraven & Martini, 1995; Altermann, 1996; Sumner & Bowring, 1996; Altermann & Nelson, 1998) Campbellrand-Malmani platform was deposited on a tectonically quiescent Kaapvaal Craton. The platform is preserved over at least 190 000 km^2 (Fig. 1) and probably originally covered the entire remaining extent of the Kaapvaal Craton, > 600 000 km^2 (Beukes, 1980, 1987). The platform is up to 1·9 km thick (Fig. 2; Button, 1973; Beukes, 1987). Approximately 500 km^2 of basinal sediments are preserved near Prieska (Fig. 1; Beukes, 1987). Although some geologists have interpreted these deposits as peritidal (Altermann & Herbig, 1991; Hälbich *et al.*, 1992), the facies are more consistent with a deep-water depositional environment, as discussed below. Carbonate deposition on the platform ended with a major transgression with deep subtidal carbonate facies deposited across the entire platform (Beukes, 1987). These grade upwards into the earliest Palaeoproterozoic Kuruman and Penge iron formations, which conformably overly the Campbellrand and Malmani subgroups.

Subsidence creating accommodation space for the platform was probably thermal cooling after an ultrahigh temperature event in the lower crust associated with the 2715 Ma Ventersdorp Supergroup lava extrusion (Armstrong *et al.*, 1991; Schmitz & Bowring, 2003a,b). Temperatures peaked at > 1000 °C at about 2720–2715 Ma (Schmitz & Bowring, 2003b). This event was associated with some rifting, as demonstrated by the presence of syneruption grabens associated with Ventersdorp lavas and thickening of the Ventersdorp Supergroup towards the western edge of the craton (Tinker *et al.*, 2002). However, sediments above the Ventersdorp Supergroup consist of mixed siliciclastic and carbonate sequences of the Schmidtsdrif Subgroup and the Wolkberg Group, lack evidence of rifting and do not show a typical passive margin geometry (Button, 1973; Beukes, 1977; Tyler, 1979; Beukes, 1983, 1987; Clendenin *et al.*, 1991). The Schmidtsdrif Subgroup sediments deepen and thicken to the south-west and west (Beukes, 1977; Tinker *et al.*, 2002), indicating a south-western margin, but a sediment source from the south-west was also present (Beukes, 1977). The Wolkberg Group is preserved in broad folds, and isopach maps demonstrate that it filled local topographic lows with the style of an intracratonic basin rather than a passive margin (Button, 1973; Clendenin *et al.*, 1991). Folding of the Wolkberg Group preceded transgression of the Kaapvaal Craton at the base of the Campbellrand-Malmani carbonate platform. The Black Reef Formation overlies these and older rocks with an angular unconformity (Clendenin *et al.*, 1991;

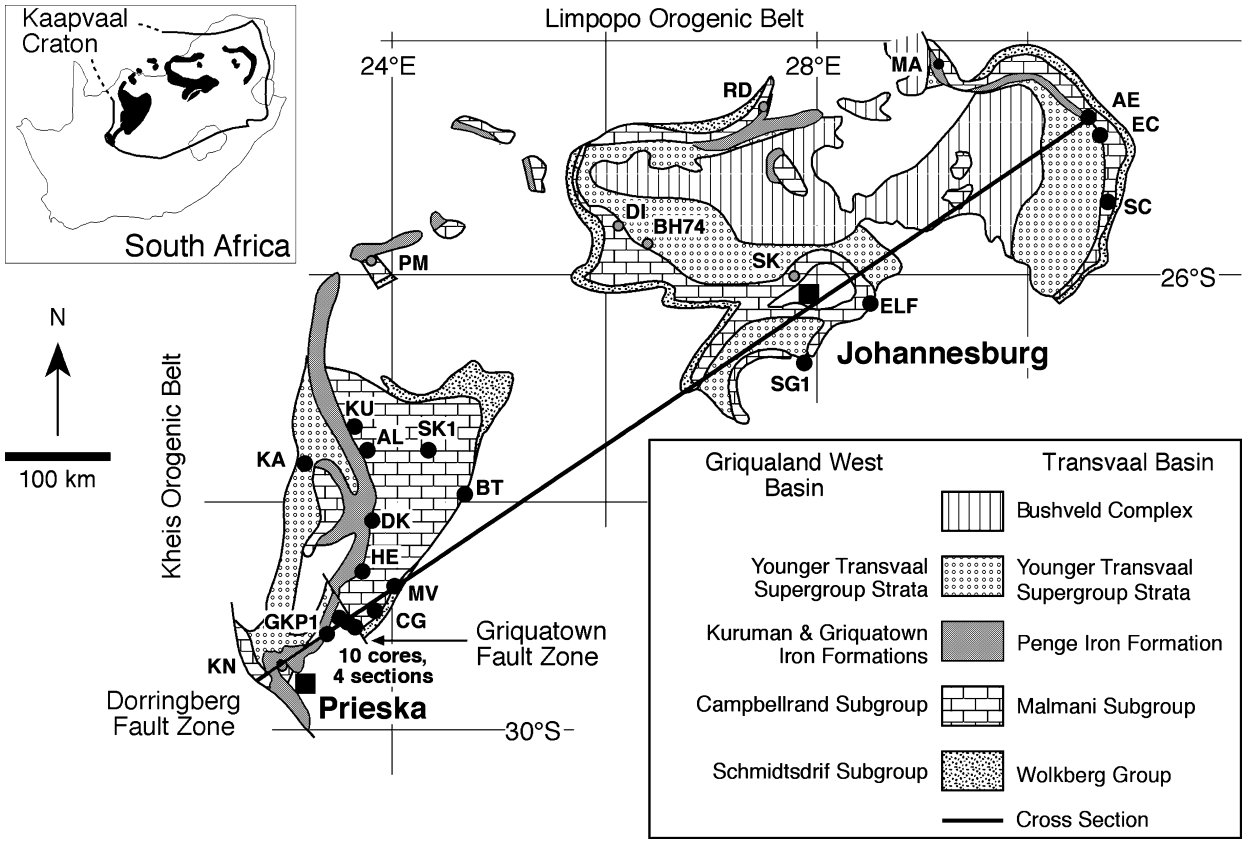

Fig. 1. Map showing the distribution of the Campbellrand-Malmani carbonate platform on the Kaapvaal craton. Circles represent the locations of measured sections or logged cores. Black circles represent sections shown in Fig. 2. Grey-filled circles represent measured sections and cores used for facies analysis, but not logged for the proportions of *in situ* precipitated carbonate and not shown in Fig. 2.

Tinker *et al.*, 2002), demonstrating regional peneplanation before transgression and initiation of carbonate sedimentation. Thus, the Campbellrand-Malmani carbonate platform was deposited on a craton lacking evidence for recent rifting to supply passive margin thermal subsidence. Rather, accommodation space may have been provided by craton-wide subsidence resulting from cooling of the lower crust, enhanced by sedimentary loading. This interpretation is consistent with the uniform thickness of the Campbellrand-Malmani carbonate platform across its preserved extent (Fig. 2; Button, 1973; Beukes, 1980, 1987; Tinker *et al.*, 2002), with the exception of much younger erosional truncation.

The Campbellrand-Malmani carbonate platform is extremely well preserved. Structural disruption of preserved strata is limited to gentle warping over most of the craton with locally steeper dips around the Bushveld Complex and folding and faulting in the Kheis Belt and Dooringberg Fault Zone, coincident with the western boundary of the Kaapvaal craton (Fig. 1; Stowe, 1986; Beukes & Smit, 1987). Faulting near Prieska along the trend of the platform margin complicates correlations between platform and basinal sediments. Much of the platform was eroded away in the south and east with progressively more of the platform preserved approaching the northern and western edges of the preserved basin (Button, 1973; Beukes & Smit, 1987). Metamorphic alteration has been limited with most outcrops below greenschist facies metamorphism (Button, 1973; Miyano & Beukes, 1984). Locally, amphibole is present as a result of Bushveld contact metamorphism in the Malmani Subgroup, and supergene alteration during late fluid flow produced local Pb–Zn, fluorite and gold deposits in both the Malmani and the Campbellrand subgroups (e.g. Martini, 1976; Clay, 1986; Duane *et al.*, 1991). Early, fabric-retentive dolomite replaced most of the Malmani Subgroup, particularly peritidal facies, which are also associated with chert replacement (Button, 1973; Eriksson *et al.*, 1975, 1976). However, significant amounts of the Campbellrand Subgroup still consist of limestone

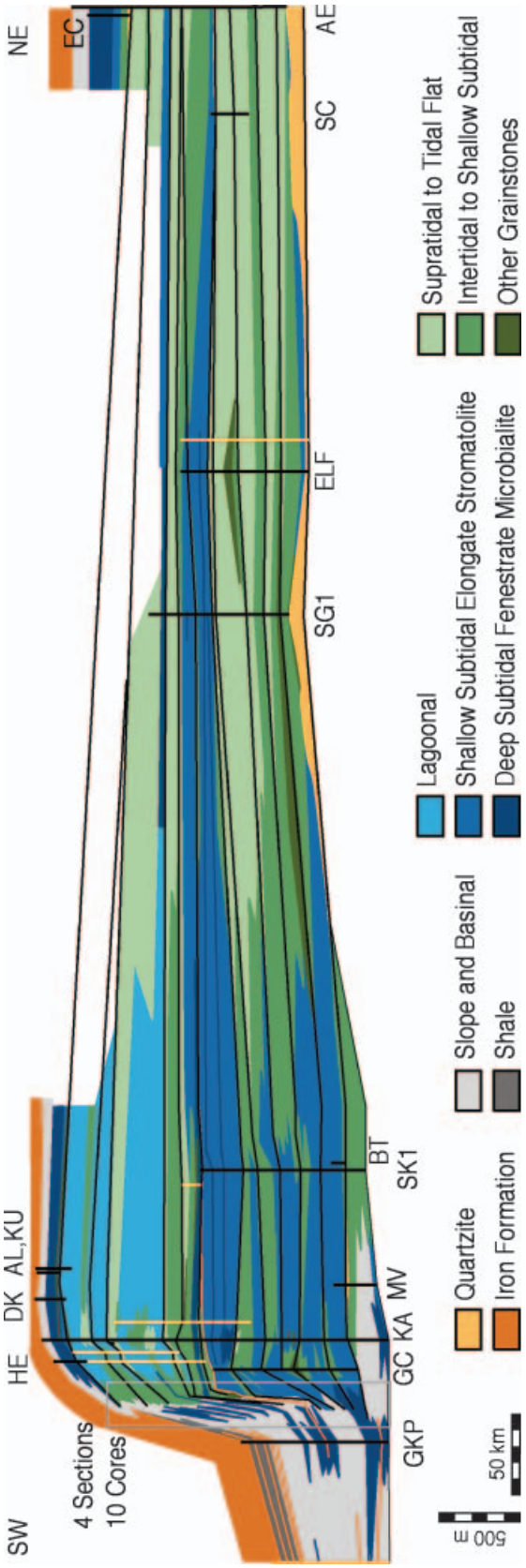

Fig. 2. Cross-section of the Campbellrand-Malmani carbonate platform. Vertical black lines show representative measured sections measured for this study; vertical orange lines in the Northern Cape Province represent sections from Beukes (1980) that were walked to evaluate facies assemblages; the vertical orange line near Johannesburg represents sections from Eriksson & Truswell (1974) that were used for facies evaluation. Abbreviated names of sections correspond to locations shown in Fig. 1. Sequence boundaries are represented by black lines. See Sumner (1995) for measured stratigraphic sections and section locations. Data from Button (1973), Eriksson & Truswell (1974), Beukes (1980) and Clendenin (1989) were also used in compilation of the cross-section.

(Beukes & Smit, 1987). Late-stage dolomitization commonly affected initially porous facies resulting in poor fabric preservation.

METHODS

Standard stratigraphic and petrographic methods were used. In addition, the best preserved sections were chosen to document the abundance of *in situ* precipitated calcite and aragonite. One or more sections with the highest proportion of continuous exposure and textural preservation were identified for each facies association. These sections were remeasured, and detailed logs of the proportion of the rock containing preserved crystallographic textures or sedimentary features implying *in situ* precipitation of either aragonite or calcite were recorded for each bed greater than 5 cm in thickness (Fig. 3). In addition, the proportion of clastic carbonate textures, the abundance of shale and the extent of chert replacement were recorded. In most cases, a

Fig. 3. Sample stratigraphic column from section BT showing the logged proportions of sediment type. 'Sand' represents the proportion of rock that consists of visible carbonate grains of sand size. 'Micro.' represents the proportion of microspar to silt-sized crystals in the rock. Much of this sediment occurs within stromatolites and could have been either transported silt-sized carbonate or carbonate that precipitated within microbial mats. 'Precip.' represents the proportion of the rock that contains preserved cement-like crystal textures. It includes both fibrous calcite and pseudomorphs after fibrous and bladed aragonite. The numbers beside and below stromatolites represent the heights and diameters of the stromatolites, respectively, in centimetres. The numbers beside fanning aragonite pseudomorphs represent the heights of the fans in centimetres.

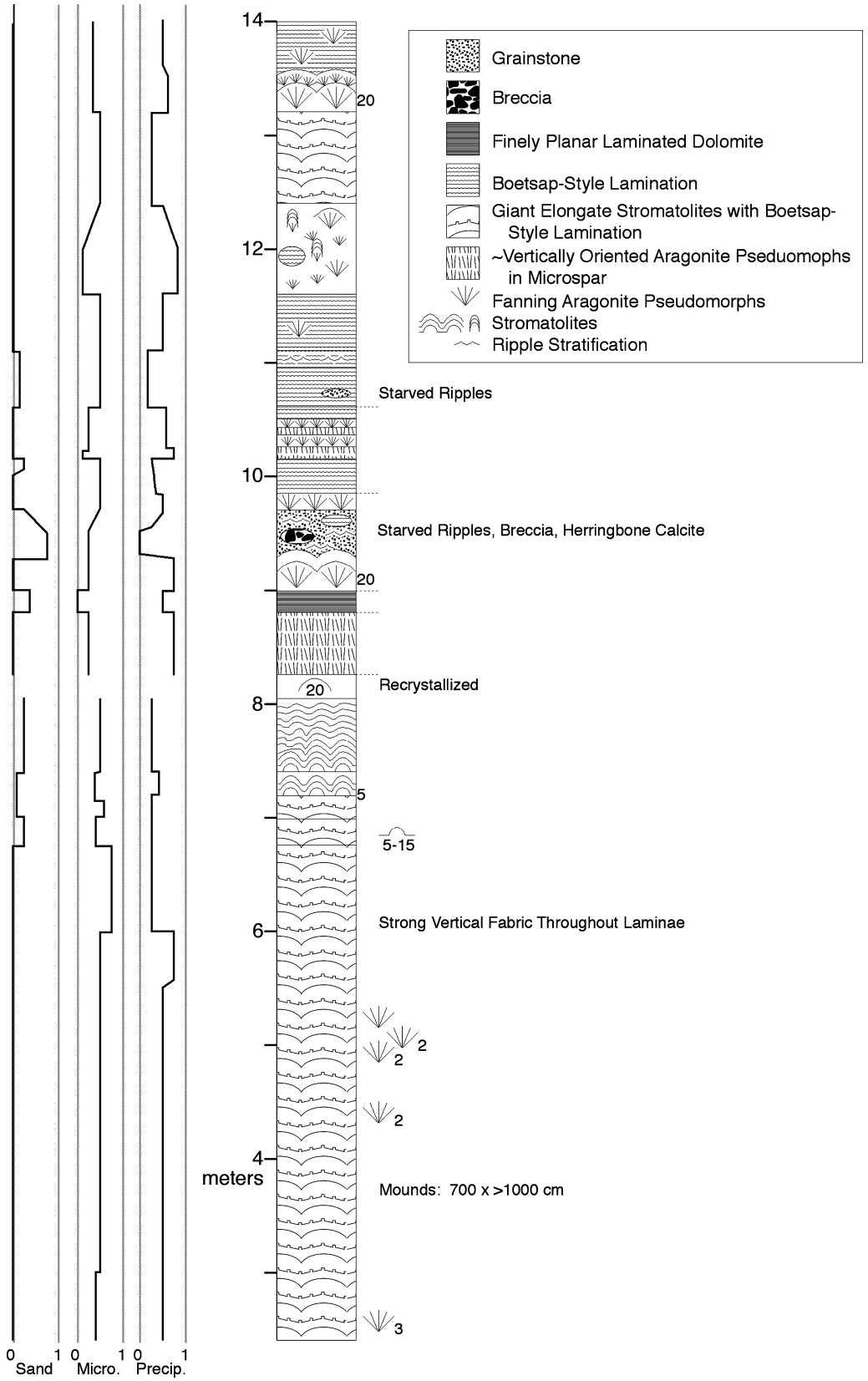
Grainstone
Breccia
Finely Planar Laminated Dolomite
Boetsap-Style Lamination
Giant Elongate Stromatolites with Boetsap-Style Lamination
~Vertically Oriented Aragonite Pseudomorphs in Microspar
Fanning Aragonite Pseudomorphs
Stromatolites
Ripple Stratification
14
12
10
8
6
4
meters
20
20
20
5
5-15
2
2
2
3
Starved Ripples
Starved Ripples, Breccia, Herringbone Calcite
Recrystallized
Strong Vertical Fabric Throughout Laminae
Mounds: 700 x >1000 cm
0 1 0 1 0 1
Sand
Micro.
Precip.

significant remainder of the rock consists of recrystallized carbonate of unrecognizable origin or depositional textures of ambiguous origin. Thus, estimates of recognized carbonate textures represent minimum proportions because part of the recrystallized or ambiguous carbonate could have precipitated *in situ* or originally been composed of grains. It is often impossible to identify the origin of all components of the rock, and the sum of the proportion that precipitated in place and the proportion consisting of clastic carbonate rarely exceeds 50%; the reported proportion of each texture represents a minimum estimate, and actual proportions are likely to be higher. For example, if the estimated composition of a bed is 25% precipitated in place and 40% clastic, up to 60% of the bed may have precipitated in place or up to 75% of the bed may have been deposited as clastic carbonate. This method provides conservative estimates of the proportions of different sedimentary components.

The average proportion of *in situ* precipitated calcite and aragonite in each lithofacies assemblage was compiled by averaging the bed-by-bed estimates over at least 10 m of section and reflects both the abundance of locally precipitated crystals and the proportions of different sedimentary components within the section. These estimates have significant errors due to variations in the proportions of different components along strike and vertically. However, they illustrate the relative importance of *in situ* aragonite and calcite precipitation in different environments on the platform, and document the overall importance of *in situ* carbonate precipitation as a platform-building process.

LITHOFACIES

Preserved lithofacies in the Campbellrand-Malmani platform range from supratidal to basinal (Fig. 2) and contain varying amounts of clastic and encrusting carbonate. The common theme to each of these assemblages, with the exception of slope and basinal lithofacies, is the evidence for calcite and, in shallow facies, aragonite crystal growth directly on the seafloor. The importance of this process differentiates Neoarchaean carbonate facies from younger carbonates even though many of the physical depositional processes were similar. The following description of lithofacies assemblages focuses on documenting the styles of *in situ* carbonate precipitation and emphasizes the differences rather than the similarities between carbonate facies in the Campbellrand-Malmani carbonate platform and more familiar younger facies.

Six lithofacies assemblages have been defined for the Campbellrand-Malmani carbonate platform. The facies are grouped by depositional environment as reconstructed from sedimentary structures and stratigraphic setting. They include: (1) supratidal to tidal flat facies; (2) intertidal to shallow subtidal lithofacies; (3) lagoonal lithofacies; (4) shallow subtidal elongate stromatolite facies; (5) deep subtidal fenestrate microbialite facies; and (6) slope and basinal facies. In addition, significant parts of the platform consist of heavily dolomitized grainstones with only rare sedimentary structures. In many cases, the depositional environments of these grainstones have not been constrained because of poor preservation of primary features.

Supratidal to tidal flat lithofacies assemblage

The supratidal to tidal flat lithofacies assemblage consists of domal stromatolites, grainstones with and without ooids, intraclast breccias, aragonite and evaporite mineral pseudomorphs and micrite.

Stromatolites

Domal stromatolites with diameters of 50–100 cm and up to 40 cm of synoptic relief are characteristic of peritidal deposits. Many of the domes are composite and contain smaller secondary domes that range from < 1 to 10 cm in diameter (Fig. 4). They nucleated on flat to irregular surfaces, including intraclasts. Commonly, domes are truncated by erosional surfaces overlain by breccias and grainstones. Domes contain four styles of lamination: bumpy colloform, smooth colloform, smooth deformed and peaked laminae. Bumpy colloform laminations (Fig. 4a) consist of pairs of ≤ 0·1 mm thick, dark red–orange lamellae and ≤ 0·5 mm thick light orange lamellae. Lamellae isopachously coat millimetre-scale irregularities on the larger stromatolites producing composite domes with occasional overhanging sides. Bumpy colloform laminae also grew downwards from the bottom of platy intraclasts as linked minidomes, 1–8 mm in diameter. Smooth colloform laminae (Fig. 4b) also consist of 0·1 mm thick dark red–orange lamellae and 0·5 mm thick light orange lamellae. Commonly, laminae are truncated at the edges of domes, and lighter colour lamellae occasionally thicken and thin across domes. Smooth colloform laminae also form overhanging

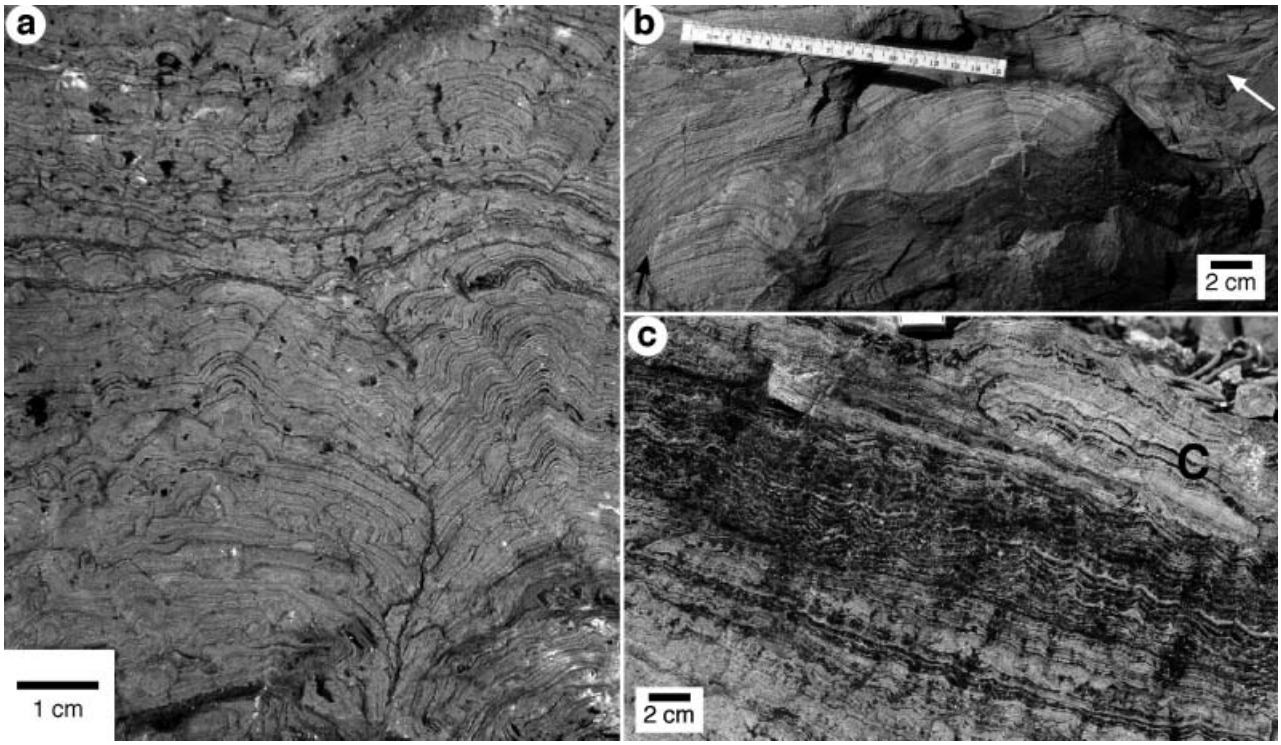

Fig. 4. Stromatolitic lamination styles in the supratidal to tidal flat lithofacies assemblage. (a) Bumpy colloform domal stromatolites contain light–dark pairs of laminae. Stromatolite morphology is highly influenced by local bumps that are isopachously coated by successive laminae. (b) Smooth deformed stromatolitic laminae show a consistent direction of deformation, which is to the right in this photograph. The trough in a small syncline is filled with grainstone (white arrow). These stromatolites also contain abundant truncation surfaces (black arrow). (c) Peaked laminae commonly pinch and swell from the tops to the sides of domal stromatolites, suggesting a significant component of transported sediment. However, laminae also isopachously coat irregularities on the surface such as clasts (C), which demonstrates the presence of either a significant component of *in situ* carbonate precipitation or sediment binding by a microbial mat. Early cementation is also demonstrated by the presence of clasts containing peaked laminae (C).

composite domes on stromatolites, but they lack millimetre-scale topographic irregularities. Occasionally, smooth colloform laminae are intercalated with abundant pods and lenses of grainstone (Fig. 4b). Smooth, deformed laminae (Fig. 4c) are composed of 0·2–1·0 mm thick pairs of grey and light orange lamellae that thin on the sides of domes where they are inclined up to 80°. Millimetre- to centimetre-thick lenses of cross-stratified grainstone are common between flat-lying laminae. Broken and folded lamellae are common in the interiors of domes, and overlying laminae seal the microfaults demonstrating that deformation occurred during growth of the dome. Commonly, deformation is accompanied by syn-sedimentary disintegration of laminae associated with fluid escape structures. Peaked laminae (Fig. 4c) consist of 0·1 mm thick dark red–orange lamellae and 1·0 mm thick light orange lamellae that are often replaced by chert. They form 5 mm wide and 10 mm high peaks with high inheritance. Peaked laminae coat intraclasts and commonly thicken into troughs, usually with an increase in the number of laminae.

The lateral continuity and even thickness of dark red and light orange lamellae and their downward growth on the undersides of clasts suggest that they grew as microcrystalline crusts that precipitated within a microbial mat. However, some of the light orange lamellae are associated with lenses of grainstones in troughs, implying that they may also contain a detrital, trapped-and-bound micrite component. Grey lamellae in deformed domes are more laterally cohesive than light lamellae in the same dome and are also present on steep slopes on the sides of domes. They are interpreted as more firmly bound micrite than the light orange layers or as precipitated microcrystalline crusts within a microbial mat. Variations in the overall morphology of the

laminations are probably due to changes in influx of detrital micrite and carbonate sand, scouring by strong currents, mat growth and precipitation within the mat. The smooth colloform stromatolites may be scoured as demonstrated by the truncation of lamellae on the edges of troughs. The crests in peaked laminae may be enhanced by sediment transport or could reflect microbial growth structures.

Wavy-laminated dolomite

Wavy-laminated, light grey dolomite contains centimetre-thick laminae that are defined by diffuse orange bands. Sedimentary structures are rare, but beds pinch over topographic highs and swell in lows, suggesting that this facies consisted predominantly of clastic carbonate. Wavy-laminated dolomite occasionally contains wave ripples and is commonly interbedded with carbonate sands and domal stromatolites within the supratidal to tidal flat lithofacies assemblage. The paucity of sedimentary structures could result from fine grain size and low-energy depositional environments or fabric loss during dolomitization. Original grain size was probably silt with minor micrite and fine sand-sized grains.

Grainstones, micrite and breccia

Grainstones and dolomicrite form < 30 cm thick beds and lenses and are usually interbedded with wavy-laminated dolomite and domal stromatolites. Wave and interference ripple stratification, mud cracks, mud chip intraclasts and channels are present. Also, tepee structures extend up to 1 m high (Button, 1973; Eriksson & Truswell, 1974; Eriksson, 1977). Platy to equant intraclasts that range in size from a few millimetres to > 70 cm long are very common as single clasts between stromatolites, in lenses of breccia and in ≤ 1 m thick breccia beds. Breccias commonly contain rip-ups of associated stromatolites ('stromatoclasts' of Sami & James, 1994) and micritic layers. Imbricated clasts with a carbonate sand matrix are common and form rosettes (Fig. 5a). Clasts associated with colloform stromatolites are commonly coated with laminae identical to that in the stromatolites, and clasts sometimes act as nuclei for new domes.

Beds of micrite and recrystallized micrite are rare. In most cases, recrystallization was extensive enough that it is hard to distinguish between fine sand- to silt-sized grainstones and possible micritic sediment. The rare beds that remain microcrystalline are typically several centimetres thick and unlaminated. They are usually associated with halite pseudomorphs, microbreccias and possible karstic dissolution surfaces. In general, they are associated with the shallowest water sedimentary structures or evidence of evaporitic concentration of sea water.

Aragonite pseudomorphs

Layers of radiating crystal pseudomorphs, 3–30 cm thick, are preserved in chert and occasionally dolomite (Fig. 5b). These pseudomorphs nucleated as botryoids on the seafloor and grew upwards in a radiating fan-like pattern. Where botryoids nucleated close together, growth of neighbouring botryoids interfered, and only the most upright crystals continued growth, thus creating a fringe of crystals oriented perpendicular to bedding. Preservation of crystal fans in the supratidal to shallow intertidal lithofacies assemblage is too poor to allow direct identification of precursor mineralogy, but similar crystal pseudomorphs, interpreted as neomorphosed aragonite, are common in intertidal to shallow subtidal deposits of the Campbellrand-Malmani platform (described below; Sumner, 2000).

Beds of flat-lying, < 1 mm thick laminae commonly contain pseudomorphs of crystals that were elongated perpendicular to bedding. Occasionally, hints of fibrous crystals extend through multiple laminae (Button, 1973; Eriksson, 1977). These fibrous crystal traces are always oriented perpendicular to bedding, and are similar to the dolomitized crystal fans, but with laminated sediment between elongate crystals. This lithofacies probably originally consisted of upward-growing aragonite crystals around which fine-grained carbonate was deposited (Sumner, 2001).

Halite pseudomorphs

Rare, 1 cm cubic pseudomorphs consisting of chert or void-filling dolomite cement are present in some micrite layers (Fig. 5c). The cubic geometry of the pseudomorphs implies the former presence of halite that grew displacively in micrite similar to those observed in modern salt pans (Lowenstein & Hardie, 1985).

Herringbone calcite layers

Herringbone calcite is a Mg-calcite cement with distinctive crystallographic properties, including a light–dark serrate banding that is roughly perpendicular to crystal growth directions (Sumner & Grotzinger, 1996b). It is present in supratidal to tidal flat facies as millimetre- to decimetre-thick coatings on stromatolites, breccia

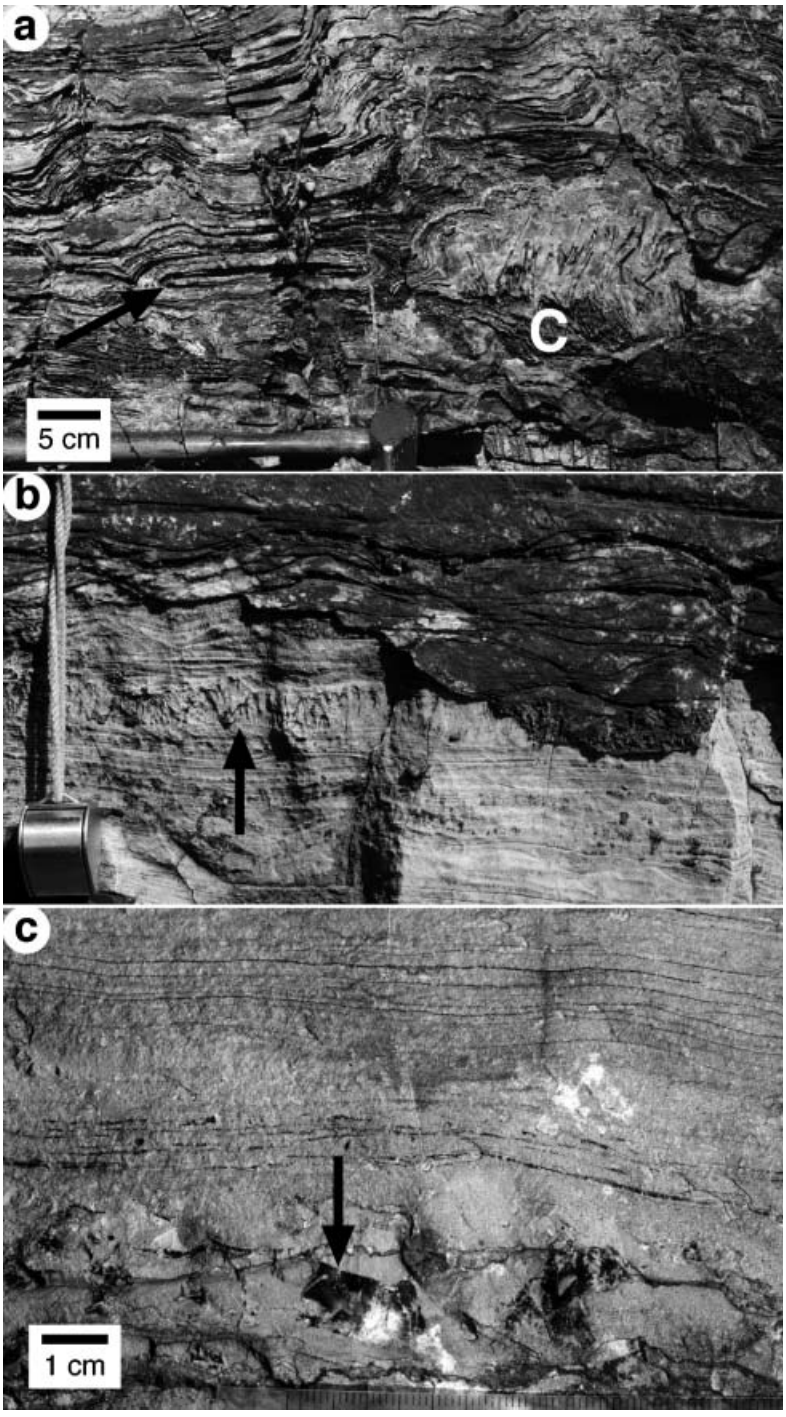

Fig. 5. (a) Rosettes of breccia clasts (C) are coated with colloform stromatolites separated by grainstone-filled troughs. Platy clasts also form the cores of oncolites (arrow). (b) Pseudomorphs of aragonite fans (arrow) are overlain by grainstone with interference ripple cross-lamination. The fans are now composed of dolomite (light) and chert (dark). The hand lens is 2 cm across. (c) Halite pseudomorphs replaced by chert (arrow) are commonly associated with micrite and wavy-laminated dolomite (top of photo).

blocks and other depositional surfaces. In one case, 50 cm long platy breccia blocks were coated by a 5 cm thick layer of herringbone calcite, rebrecciated and then recoated with another 8 cm of herringbone calcite, which cemented several clasts together. In another example, a 40 cm deep channel was coated with 10 cm of herringbone calcite at the bottom and 20 cm of herringbone calcite on the edges. Growth started on the edges before the bottom, possibly as a result of sediment transport along the floor of the channel as herringbone calcite grew on the sides. The channel was infilled with graded volcanic accretionary lapilli followed by tuffaceous sediment. Laterally, this lapilli layer overlies herringbone calcite-rich stromatolites with digitate stromatolites in the

troughs (Sumner, 1997a). Most layers of herringbone calcite, however, are thin coatings on stromatolites, and it forms a minor proportion of the average lithofacies.

Quartz sand and shales

Very rare quartz sandstones, siltstones and shales are associated with exposure surfaces in the supratidal to tidal flat lithofacies assemblage. The quartz arenites are fine- to coarse-grained and are chemically and physically mature. Cross-stratification consists of small-scale trough cross-bedding, wave and current ripple stratification and low-angle truncations. Shales and siltstones are usually exposed poorly, and sedimentary structures are hard to identify. Rare current-rippled grainstones are interbedded with some shales, and Button (1973) reported some ripples in siltstones. Overall, the assemblage of observed cross-stratification styles is consistent with shallow subtidal to supratidal depositional environments. Quartz arenites, siltstones and shales commonly overlie sequence boundaries, consistent with shallow depositional environments.

Interpretation of lithofacies assemblage

Sedimentary structures, including erosional channels, wave and interference ripples, abundant imbricated intraclasts, mudcracks, tepee structures and rare evaporite pseudomorphs, support a shallow intertidal to supratidal depositional environment for this lithofacies assemblage. This interpretation is consistent with previous interpretations of composite domal stromatolites as shallow intertidal to supratidal stromatolites (e.g. Grey & Thorne, 1985; Hoffman, 1988).

Calcite and aragonite precipitation both occurred in supratidal to tidal flat depositional environments although dolomitization obscured many primary textures. Based on detailed logging of 140 m of exposed section at SC, a minimum of 10% of the rock precipitated in place, mostly as fine-grained carbonate within stromatolitic mats. The original mineralogy of most precipitates is unknown. However, botryoidal aragonite pseudomorphs are present, and thick coatings of herringbone calcite demonstrate that precipitation also occurred outside of stromatolitic mats, although these precipitates are volumetrically insignificant (< 1% of rock volume for both). At least 55% of the rock was deposited as clastic carbonate, including ooids, and the remaining 35% is of unknown origin.

Intertidal to shallow subtidal lithofacies assemblage

The intertidal to shallow subtidal lithofacies assemblage is dominated by columnar stromatolites, but also contains oolitic and non-oolitic grainstones and decimetre-tall fans of aragonite pseudomorphs.

Stromatolites

Columnar stromatolites form beds up to several metres thick as well as isolated bioherms up to 1 m in diameter. Bioherms are commonly developed on unconformities and are overlain by grainstones. Individual stromatolites, usually 1–20 cm in diameter, show a variety of branching patterns and wall structures (Fig. 6a). Many of the columnar stromatolites at section BT were classified as belonging to the groups *Topinamboura*,

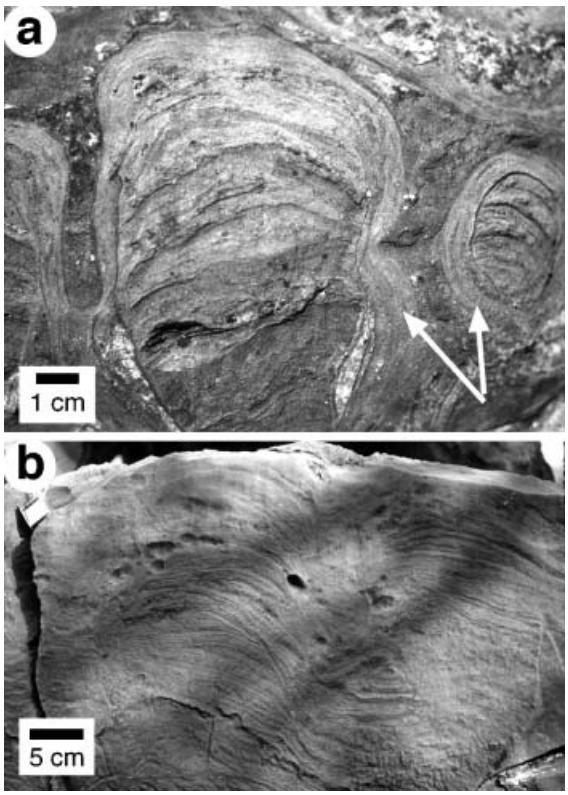

Fig. 6. (a) Columnar stromatolite composed of slightly recrystallized fibrous calcite crystals, secondary dolomite and organic inclusions is coated with a thick layer of fibrous aragonite pseudomorphs preserved as calcite (arrows). The final fill between columns consists of coarsely crystalline dolomite interpreted as originally grainstone. (b) Trapped and bound stromatolites have an irregular morphology and are composed of coarsely crystalline dolomite. Laminae are commonly truncated by erosion surfaces.

Radiatina, *Katernia*, *Pilbaria*, *Tibia* and *Sapinia* (Bertrand-Sarfati & Eriksson, 1977), and similar morphologies are present in the columnar stromatolite-dominated lithofacies assemblage throughout the platform. The microtexture of many of the columnar stromatolites consists of vertically oriented elongate crystals and fine, filmy laminae defined by organic inclusions (Bertrand-Sarfati & Eriksson, 1977). The crystals are composed of fibrous calcite and Mg-calcite that grew upwards. Some columns have a herringbone calcite microtexture (Sumner & Grotzinger, 1996b).

Rare irregular decimetre-scale domal stromatolites are also present (Fig. 6b). These domes are dolomitized and contain centimetre-thick laminae that pinch and swell and are truncated along abundant micro-unconformities. They have low inheritance. Lenses of grainstone are common between and within domes. The pinching, swelling and truncation of laminae as well as the abundance of associated grainstone suggest that these domes formed by trapping-and-binding of coarse-grained sediment.

Aragonite pseudomorphs

Fanning crystal pseudomorphs grew off the sides of columnar stromatolites and upwards from bedding surfaces (Fig. 7; Sumner & Grotzinger, 2000). They consist of bundles of fibrous crystals that grew upwards in a radial pattern from a single point and reach heights of over 50 cm. Commonly, they are draped by sediment and form domes geometrically similar to stromatolites. Rare fan layers contain no clastic carbonate between pseudomorphs, in which case void space between fans is filled with herringbone calcite and other fibrous precipitated calcite. Neighbouring fans commonly intersected each other as they grew, and the most inclined bundles of crystals abut each other (Sumner & Grotzinger, 2000).

The exclusively upward growth of fanning fibres, their presence in beds lacking detrital carbonate and the presence of shelter porosity under steeply inclined pseudomorphs all suggest that the fans grew directly on the seafloor and not as diagenetic crystals within the sediment (Sumner & Grotzinger, 2000). The petrographic characteristics of the fans, including fibrous crystal morphology, flat irregular crystal terminations, pseudohexagonal cross-sections of fibre bundles and the optically unoriented, elongate secondary calcite crystals that cross-cut primary crystal boundaries, are consistent with an aragonite precursor mineralogy (Sumner & Grotzinger, 2000).

Oolitic grainstones

Oolites are abundant in the north-east and are less common elsewhere in the platform. Ooids are commonly mixed with non-oolitic sand and are also present in lenses and troughs associated with stromatolites. In the north-east, beds and lenses of oolite are usually graded either normally or inversely. Normally graded beds are interpreted as representing deposition in a waning flow. Inversely graded beds commonly range in grain size from very fine sand to 3 mm diameter ooids (Fig. 8). Inverse grading is interpreted as the

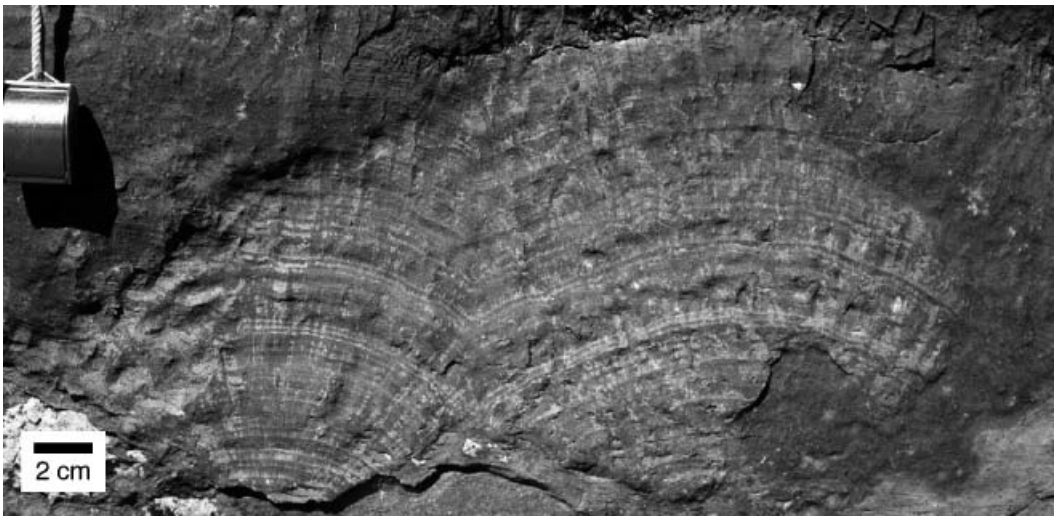

Fig. 7. Fanning aragonite pseudomorphs draped by fine-grained carbonate sediment. The upper surface of this bed is domed above each fan of pseudomorphs.

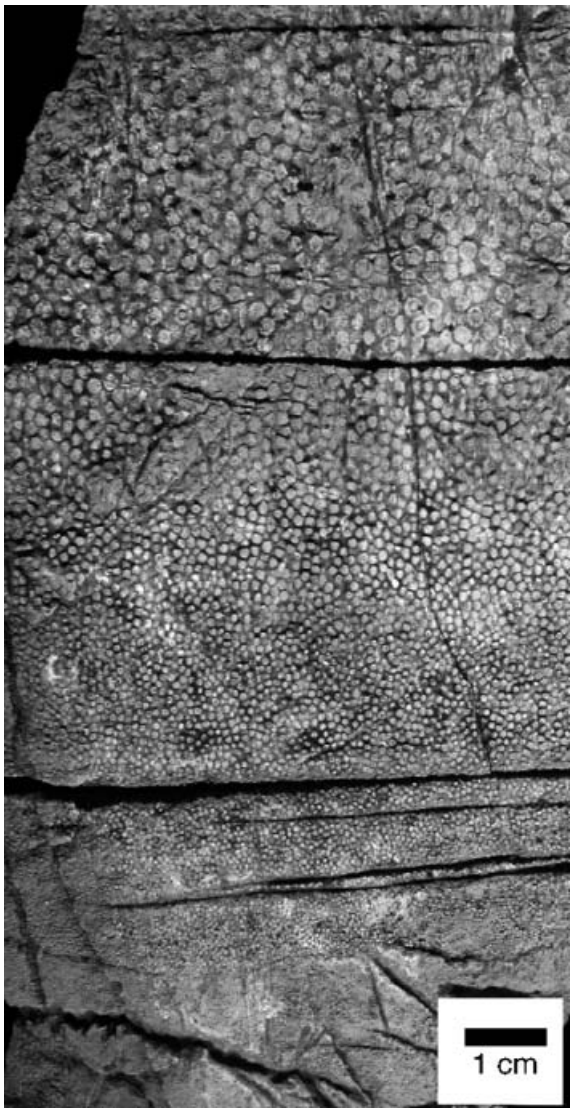

Fig. 8. Inversely graded ooids from section AE range in size from very fine to very coarse sand. Inversely graded oolites lacking cross-stratification are common in the intertidal to shallow subtidal lithofacies assemblage.

result of a single influx of ooid nuclei that were coated and progressively buried as they grew. Ooids remaining on top continued to grow resulting in the largest ooids at the tops of the beds (see Sumner & Grotzinger, 1993). Wave and interference ripples are present in rare ungraded oolite beds. Large-scale cross-stratification was not observed, even in sections containing abundant ooids, suggesting the absence of large oolitic bedforms and shoals. The characteristics of inversely and normally graded beds and beds with shallow water ripple stratification suggest that the oolites formed on tidal flats and in shallow subtidal depositional environments that were agitated frequently enough to produce well-rounded grains.

Other grainstones

Dolomitized non-oolitic grainstones form lenses and thin beds containing wave ripple, current ripple and low-angle cross-stratification. Commonly, they are present in troughs between columnar stromatolites and fill topography created by stromatolite beds and bioherms. Lenses and thin beds of intraclast breccia also are present, especially overlying erosionally truncated columnar stromatolites.

Interpretation of lithofacies assemblage

The abundance of unconformities, rare channelling, the presence of ripple, small dune and low-angle cross-stratification in grainstones and the 1 m synoptic relief of bioherms suggest a lower intertidal to shallow subtidal depositional environment for the lithofacies assemblage.

The proportion of *in situ* precipitation was not adequately logged to estimate an overall proportion of precipitated textures in the intertidal to shallow subtidal lithofacies assemblage. The diversity of textures and proportions of grainstones makes estimates from a single area unlikely to reflect average percentages for the facies overall. Some parts of sections contain large proportions of precipitated stromatolites (over 75%), whereas other parts of sections in similar depositional environments contain predominantly grainstones or trapped and bound stromatolites. Thus, the proportion of this facies that precipitated in place as crystals on the seafloor is extremely heterogeneous, and additional characterization is needed to provide a quantitative estimate.

Lagoonal lithofacies assemblage

The lagoonal lithofacies assemblage contains fenestral, microbial mat laminae and small domal stromatolites. The fenestral microbial laminae consist of dark, finely laminated, 5 mm thick layers of calcite that alternate with 5 mm thick white sparry calcite layers to form metre-thick beds of limestone (Fig. 9). Both dark and white layers of calcite are laterally discontinuous, and abundant erosional truncation of laminae is apparent. Rare breccias with <1 cm diameter clasts are associated with some of the truncation surfaces. White layers are coarsely crystalline, and crystals appear to have grown inwards from the top and bottom of the layers. Fine laminae within dark layers are defined by organic

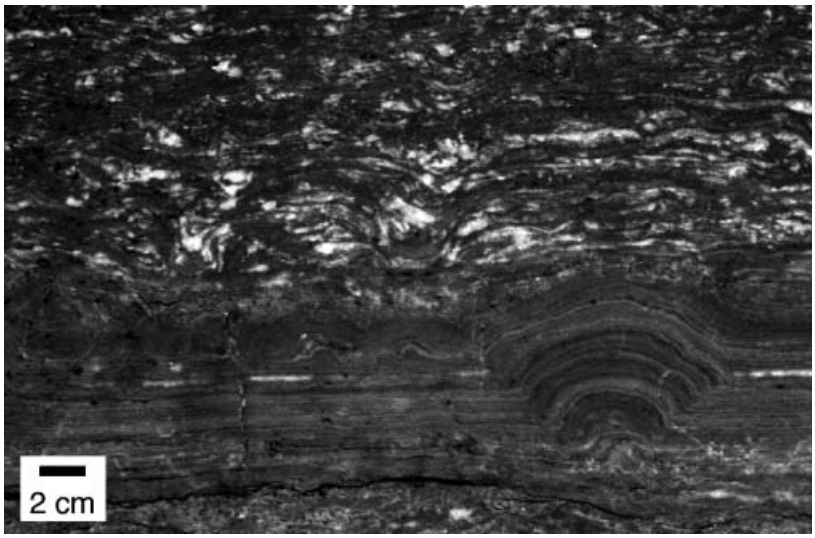

Fig. 9. Lagoonal lithofacies consist of fenestral, microbial laminae (upper half of photo) and isopachously laminated domes connected by planar laminae that are continuous with laminae in the dome.

inclusions. These laminae are interpreted as having been produced by microbial mats based on the abundance of organic inclusions and the style of the fine laminae (Beukes, 1987). White layers are probably laminae-parallel fenestrae filled with early cements (Beukes, 1987).

Light grey ≤10 cm diameter domes are interbedded with the fenestral laminite lithofacies (Fig. 9). Typically, these domes formed 5–10 cm thick beds, but beds up to 1·5 m thick are present. The hemispherical domes are laterally linked with laminae of even thickness. The domes nucleated on planar to slightly irregular surfaces that sometimes show erosional features such as truncated laminae and intraclast breccia. The domes grew upwards with isopachous laminae, a few millimetres thick, coating the initial dome. Some domes are truncated by an erosional surface, and new domes formed above them in thick beds. Alternatively, domes are overlain by fenestral laminite rocks. The domes are composed of coarsely crystalline calcite with a rare crystal elongation perpendicular to lamination. The isopachous geometry of the domes and the crystal elongation are consistent with a precipitated origin, either calcite or aragonite.

The fenestral laminite lithofacies alternates with the isopachous dome lithofacies on a decimetre to metre scale. Occasionally, several metre thick intervals of fenestral laminite lithofacies contain very poorly developed isopachous domes, and the two lithofacies are gradational into each other.

Interpretation of lithofacies assemblage

The abundance of small truncation surfaces and the lack of cross-stratification and channelling suggest a shallow subtidal depositional environment with little agitation. The stratigraphic position of these lithofacies platformward of a rimmed margin consisting of the intertidal to shallow subtidal columnar stromatolite-dominated lithofacies assemblage suggests a lagoonal depositional environment (Fig. 2; Beukes, 1987).

The proportion of the lagoonal lithofacies assemblage that precipitated as crystals directly on the seafloor depends on the relative abundance of the isopachous domes and the fenestral laminite. The isopachous domes are composed of an average of 90% carbonate that precipitated as encrustations on the seafloor. In contrast, the proportion of the fenestral laminite that precipitated on the seafloor was probably less than 10%, with at least 50% of the carbonate in the laminite precipitating below the sediment–water interface in fenestrae and within microbial mats. If only the isopachous domes and rare interbedded herringbone calcite layers and stromatolites are considered *in situ* precipitates, an average of 10% of the lagoonal lithofacies assemblage precipitated as crystals on the seafloor. If fenestrae-filling cements are included in the proportion of *in situ* precipitated carbonate, approximately 40% of the facies precipitated as crystals on or within voids below the sediment–water interface. Identifiable clastic carbonate consists of rip-up clasts of the fenestral laminite, which form significantly less than 1% of the facies. The remaining 50% of the rock probably precipitated within the sediment, including within laminated mats, leading to a tentative interpretation that essentially all the lagoonal lithofacies assemblage consists of locally precipitated carbonate. No evidence for settling of micrite from suspension was observed.

Shallow subtidal elongate stromatolite lithofacies assemblage

The shallow subtidal elongate stromatolite lithofacies assemblage consists predominantly of elongate stromatolites with variable internal textures. They have rare interbeds of rippled grainstone, breccia and flat-lying beds with aragonite pseudomorph fans. The elongate mound stromatolites range from 2 to 10 m wide and from 5 to >45 m long (Fig. 10; Truswell & Eriksson, 1972, 1973; Button, 1973; Eriksson & Truswell, 1974; Eriksson *et al.*, 1976; Eriksson, 1977; Beukes, 1987). Synoptic relief ranges from 30 to 200 cm. The mounds contain small columnar stromatolites, smooth to peaked laminae, herringbone calcite encrustations and aragonite pseudomorph fans. Some mounds show decimetre-thick cycles consisting of grainstones gradationally overlain by calcite encrustations or precipitated stromatolites.

Columnar stromatolites

Columnar stromatolites within the elongate stromatolites are 1–5 cm in diameter and have convex to rectangular laminae with a variety of branching patterns. Some of them are classified as belonging to the groups *Radiatina* and *Katernia* (Bertrand-Sarfati & Eriksson, 1977). These stromatolites contain both optically oriented crystals and silt-sized clastic grains, including rare quartz silt (Bertrand-Sarfati & Eriksson, 1977), suggesting a combined precipitated and trapped-and-bound origin for the small columnar stromatolites.

Boetsap-style lamination

Boetsap-style lamination is named after the dominant stromatolitic lamination style at Boetsap, which is the first location in which stromatolites were described from the Campbellrand Subgroup (Young, 1932). Boetsap-style lamination consists of heterogeneous combinations of dark red–brown microcrystalline carbonate lamellae, lighter red–brown to grey finely crystalline lamellae and light grey coarse sparry layers (Fig. 11a and b). Rare patches of herringbone calcite are also preserved in rocks with the Boetsap-style lamination. Boetsap-style lamination contains lamellae with more variable composition and thickness than other lamination styles described from the Campbellrand-Malmani platform. It commonly forms the internal texture of elongate mound stromatolites.

Red–brown microcrystalline carbonate lamellae consist of dolomite and vary in thickness from 1 to 3 mm along a single lamella (Fig. 11a). Commonly, their upper surfaces are peaked (Fig. 11b), similar to peaked laminae in peritidal domal stromatolites. They occasionally contain a vertical fabric suggestive of very fine, vertically oriented aragonite pseudomorphs (Fig. 11a). Red–brown microcrystalline carbonate laminae make up about 50% of a bed classified as containing the Boetsap-style lamination. Light red–brown to grey, finely crystalline lamellae are uniformly <1 mm in thickness. Grey, finely crystalline lamellae are predominantly calcite, whereas red–brown lamellae consist of dolomite. Grey and red–brown lamellae grade laterally into each other, suggesting that the red–brown lamellae are dolomitized grey lamellae. A vertical fabric is visible in thicker lamellae, and occasionally fibrous crystal pseudomorphs project through lamellae in a fan-like geometry (Fig. 11a). Grey and red–brown finely crystalline lamellae compose

Fig. 10. Giant elongate stromatolites overlain by horizontally bedded intertidal columnar stromatolites. Person for scale in circle.

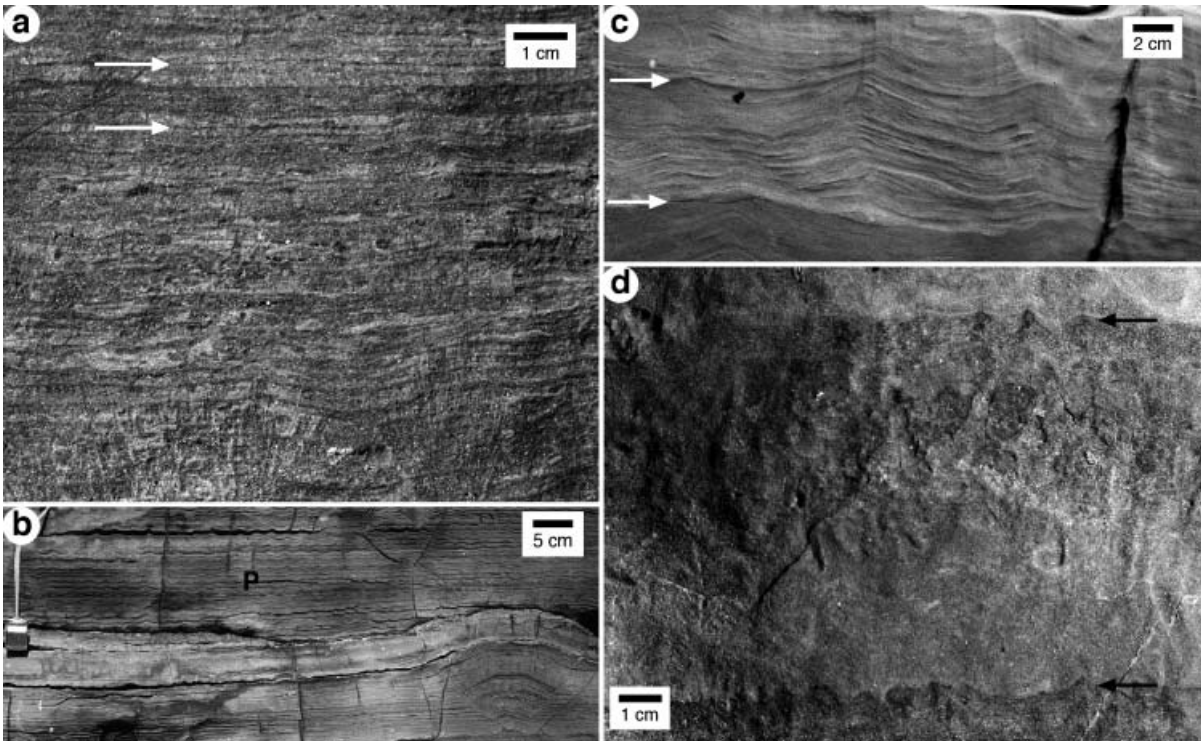

Fig. 11. Some of the internal textures in giant elongate stromatolites. (a) Boetsap-style lamellae consist of red–brown microcrystalline carbonate (thick dark bands), light red–brown to grey finely crystalline lamellae (arrows) and light grey coarse sparry layers (light, discontinuous layers). Vertical fabric, interpreted as aragonite pseudomorphs, is developed most strongly at the base of the photo, but is present throughout the field of view. (b) Isolated fans of aragonite pseudomorphs in giant elongate stromatolites grew contemporaneously with deposition of Boetsap-style laminated dolomite. Peaked laminae morphology is well developed in the upper layer (P). (c) Grainstone–cement cycles in elongate stromatolites consist of bedforms showing two directions of sediment transport that grade upwards into cement crusts. The tops of cycles (arrows) typically consist of 90% cement and are abruptly overlain by grainstones. (d) Grainstone–stromatolite cycles in elongate stromatolites also contain grainstones at their base. These develop upwards into small columnar to bulbous stromatolites. The tops of cycles (arrows) are commonly irregular, and some troughs between stromatolites are filled with grainstone.

about 50% of layers with the Boetsap-style lamination. Coarse sparry laminae consist of dolomite and vary laterally in thickness, occasionally pinching out. They are up to 1 cm thick and contain ripple stratification. Coarse sparry laminae do not contain a vertically oriented fabric and make up < 1% of laminae.

Red–brown microcrystalline carbonate layers are interpreted as dolomitized fine-grained clastic carbonate, because of their variable thickness, with a small proportion of neomorphosed aragonite represented by the vertically oriented fabric (Sumner & Grotzinger, 2000). Both red–brown and grey finely crystalline laminae are interpreted as variably altered precipitated laminae. The vertical crystal fibres that project through lamellae were probably originally aragonite (Sumner & Grotzinger, 2000). Rare herringbone calcite demonstrates that Mg-calcite also precipitated in the giant elongate stromatolites (Sumner & Grotzinger, 1996b). Coarse, sparry laminae are interpreted as recrystallized clastic carbonate deposited from tractional currents.

Aragonite pseudomorphs

Isolated crystal fans (Fig. 11b) and continuous layers of crystal fans are present within the giant mound stromatolites. These fans have the same characteristics as those in the columnar stromatolite-dominated assemblage, including crystallographic characteristics suggesting an aragonitic primary mineralogy (Sumner & Grotzinger, 2000).

Cement cycles

Giant mound stromatolites at the base of the Gamohaan Formation (Fig. 2) contain 3–10 cm thick cyclic beds with basal light tan grainstones that grade upwards into calcite cement crusts with less than 10–25% clastic carbonate (Fig. 11c and d; Sumner, 1997a). Some grainstones contain

centimetre-high bedforms showing bidirectional sediment transport. The grainstones grade upwards into either herringbone calcite crusts with a laterally uniform thickness or columnar stromatolites 3–5 cm in diameter (Fig. 11d; Sumner, 1997a). The stromatolites are poorly laminated and often contain a herringbone calcite microtexture. They widen upwards leaving teardrop-shaped troughs that are filled with the basal grainstone of the overlying bed. The tops of cycles are sometimes scoured and marked by irregular truncation surfaces (Sumner, 1997a).

Interpretation of lithofacies assemblage

Giant elongate mound stromatolites are common in Precambrian carbonate platforms, and above wave base, open-marine subtidal depositional environments for them have been well established (e.g. Hoffman, 1969; Button, 1973; Truswell & Eriksson, 1973; Eriksson & Truswell, 1974; Grotzinger, 1986; Pelechaty & Grotzinger, 1988). The characteristics of the giant mound stromatolite lithofacies assemblage and its stratigraphic distribution in the Campbellrand-Malmani platform support this interpretation.

The proportions of *in situ* precipitated and clastic carbonate in the elongate stromatolite lithofacies assemblage were evaluated in 18 m of section at SC, 33 m of section at BT and 14 m of section at KU. The minimum proportions of carbonate that precipitated directly on the seafloor range from 20% (SC) to 35% (BT and KU). Minimum clastic carbonate proportions are 10% (BT), 20% (KU) and 30% (SC), leaving approximately half the rock of unknown origin. The three sections characterized are dominated by different stromatolitic textures in the mounds. The section at SC was deposited in the north-east during a transgression. Internal textures are dominated by peaked laminae with a significant component of fine clastic carbonate. Some of the giant mounds in section BT, also deposited during a transgression, contain similar internal textures, but aragonite pseudomorphs are locally abundant. The preservation of internal textures is better at BT than in other sections, and more precipitated textures could be identified within the peaked laminae that contain some clastic carbonate. In contrast, section KU is dominated by cycles of grainstone to stromatolites or calcite crusts. Aragonite pseudomorphs are absent, and centimetre-thick layers of herringbone calcite are abundant. No fine-grained clastic carbonate was deposited in this environment, possibly on account of higher water flow speeds. Overall, the shallow subtidal elongate stromatolite facies is variable, but contains a significant proportion of carbonate that precipitated directly on the seafloor. The abundance of decimetre-tall aragonite fans and decimetre-thick calcite encrustations demonstrates that giant mound stromatolite growth was a function of both precipitation and clastic carbonate deposition.

Deep subtidal fenestrate microbialite lithofacies assemblage

Fenestrate microbialites contain three components (Figs 12 and 13a; Sumner, 1997b, 2000): draping, mat-like laminae; vertically oriented structures called supports; and voids filled with carbonate cements. Mat-like laminae are 1 to tens of micrometres thick, very smooth and defined by organic inclusions. These laminae were flexible and laterally cohesive during growth as demonstrated by recumbent synsedimentary folding of laminae (Sumner, 1997b). Supports are 100 to >300 μm wide and commonly oriented vertically. They are interlocking surfaces in three dimensions and branch in some microbialites (Sumner, 1997b, 2000). Supports are defined by organic inclusions and are interpreted as microbial in origin because of their three-dimensional geometry and their soft, folded character in some microbialites (Sumner, 1997b, 2000).

Fenestrate microbialites are classified into seven end-member microbialite morphologies: planar laminae, contorted laminae and roll-up structures (*sensu* Simonson & Carney, 1999), tented microbialites, net-like microbialites, cuspate microbialites, irregular columnar microbialites and plumose structures (Sumner, 1997b, 2000). Beds of herringbone calcite lacking microbial structures also occur in this lithofacies assemblage. Five assemblages of microbial structures include (Sumner, 1997a): (1) the bedded cuspate microbialite assemblage consisting of interbedded cuspate microbialites, contorted laminated mat and plumose structures; (2) the planar laminated mat assemblage consisting of planar laminated mat, tented microbialites and contorted laminated mat; (3) the irregular columnar microbialite assemblage consisting of irregular columnar microbialites, contorted and planar laminated mat, plumose structures, herringbone calcite beds, cuspate microbialites and tented microbialites, in order of decreasing abundance; (4) the contorted laminated mat assemblage consisting of contorted and planar laminated mat with rare interbeds of shale and cuspate

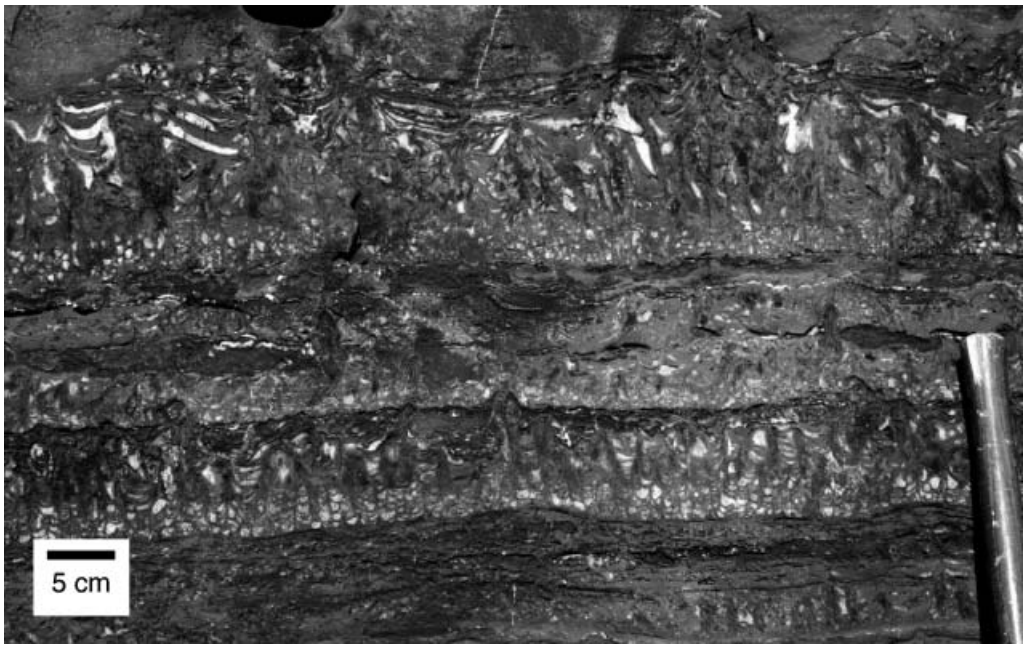

Fig. 12. Fenestrate microbialites show diverse morphologies. Cuspate microbialites with well-developed vertical supports and draping laminated mat are present in the layer above the scale bar. Layers are separated by contorted laminated mat.

microbialites; and (5) the net-like microbialite assemblage consisting of decimetre-thick cycles with net-like microbialites at the base and grainstones or columnar stromatolites at the top.

The various microbialite assemblages occur in different parts of the platform. Microbialites basinward of the platform margin consist of a mix of the bedded cuspate, irregular columnar, contorted laminated mat and net-like microbialite assemblages interbedded with organic-rich shale, slope breccia and nodular limestone and dolomite. Microbialite units deposited on top of the platform during transgressions consist exclusively of the net-like microbialite assemblage. During final drowning of the platform, fenestrate microbialites were deposited across the entire platform. In the north-east, facies consist of the bedded cuspate microbialite assemblage overlain by those of the planar laminated mat assemblage (Sumner, 1997a). In contrast, western outcrops contain abundant bedded cuspate microbialite assemblage rocks overlain by those of the irregular columnar microbialite assemblage, which is followed by rocks of the contorted laminated mat assemblage (Sumner, 1997a).

Interpretation of lithofacies assemblage

The delicate morphology of the microbialites, the lack of evidence for scouring and the absence of clastic carbonate all suggest a deep subtidal, subwave base depositional environment for the microbialite assemblages in the Gamohaan and Frisco formations and basinward of the platform margin (Beukes, 1987; Sumner, 1997a). Net-like microbialite facies were deposited on the top of the carbonate platform as wedges between facies tracts consisting of the giant stromatolite lithofacies assemblage, and are also interpreted as low-energy subtidal deposits with variable clastic carbonate influx.

The proportion of calcite that precipitated in place was logged meticulously for the fenestrate microbialite lithofacies assemblage at section KU. For the bedded cuspate microbialite and irregular columnar microbialites assemblages, $>35\%$ of the rock contains preserved crystallographic textures indicating that it precipitated as encrustations and void-filling cements (Sumner, 1997a). Thirty per cent of the void-filling cements and almost all the calcite encrustations consist of herringbone calcite, implying that a minimum of 15% of the rock precipitated as fibrous marine cement. Microcrystalline carbonate comprises 30% of the rock and is present only in areas with dense organic inclusions defining the microbial structures. Across the top of the platform, micritic beds, drapes and geopedal void fills are absent, and there are no sedimentary features suggesting that the microcrystalline carbonate originally consisted of

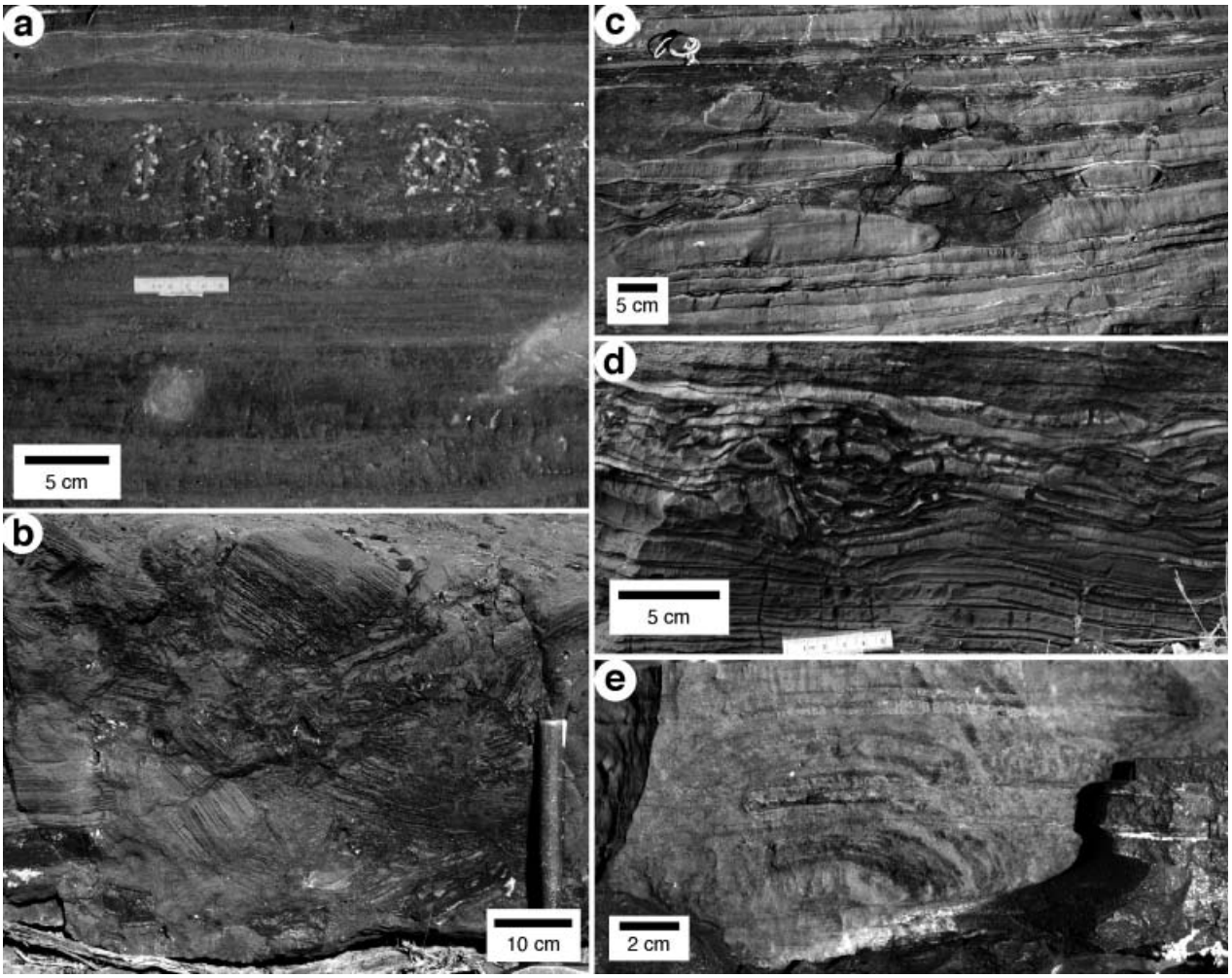

Fig. 13. Slope and basinal lithofacies. (a) Fenestrate microbialites interbedded with laminated dolomite. (b) Breccia composed of laminated dolomite clasts with a dolomite matrix. (c) Carbonate nodules in a shale-rich unit. Note the compaction between nodules. (d) Platy breccia with limestone clasts, which is interpreted as local brecciation resulting from soft sediment deformation. (e) A concretionary dome with flat-lying sedimentary laminae running through the dome. Sedimentary laminae are continuous from the dolomite (light) into secondary chert (dark).

micritic sediment (Sumner, 1997a). Rather, the concentration of microcrystalline carbonate in organic-rich areas suggests that it precipitated within microbial mats as a microsparitic cement. Even more than the 65% of the rock composed of cements and microspar probably precipitated as calcite cements and encrustations, but lacks the crystal textures required for positive identification as a result of diagenetic recrystallization. All exposed correlative stratigraphic intervals, e.g. at AL, DK, HE, and core KA, which span $\approx$7000 km^2, contain similar proportions of marine cement (Sumner, 1997a). Thus, the *in situ* precipitation of marine calcite was the most important rock-forming process in the deposition of the bedded cuspate microbialite and irregular columnar microbialite assemblages.

In the planar laminated mat assemblage, most of the carbonate consists of microcrystalline calcite encasing the remnants of microbial mats. Lenses of sediment are absent, and there is no specific evidence for an influx of clastic carbonate. However, textures implying local precipitation of calcite are rare and only associated with voids in tented microbialites. The preferred interpretation for the origin of the microcrystalline carbonate is precipitation within and on microbial mats.

The contorted laminated mat assemblage contains variable amounts of void-filling calcite cements. In areas with more abundant cuspate microbialites, void-filling cements are common. However, in deeper slope environments where shale is a larger proportion of the assemblage,

contorted laminae are only visible in precompaction carbonate concretions, implying that the calcite precipitated within the sediment.

The net-like microbialite assemblage contains some grainstone (10%) at the tops of decimetre-thick cycles. Voids rarely contain interpretable textures, but some rarely contain isopachous laminae that suggest they were filled with cements (Sumner, 2000). In most cases, textures are not well enough preserved to demonstrate the origin of the carbonate.

Slope and basinal lithofacies assemblage

Slope and basinal lithofacies are composed predominantly of the 'Prieska Facies' of Beukes (1987) and Altermann & Herbig (1991). Slope sediments mostly consist of finely planar laminated dolomite interbedded with very fine crinkly laminated dolomite. Crinkly laminae rarely dome or peak upwards with planar laminated dolomite draping topography and preferentially filling minor topographic lows. The original grain size of the sediment was fine sand or smaller based on current crystal sizes. Beds of planar laminated dolomite are sometimes folded and brecciated with folding implying westward synsedimentary slumping. Fifty to 90% of some >10 m thick intervals are composed of breccia in beds ranging from a centimetre to a metre thick. Clasts are commonly elongate, range from <1 to >10 cm in length, are unsorted and consist of laminated dolomite similar to interbedded sediments (Fig. 13b). The matrix is dolomite. Rare lenses of breccia with a sparry calcite matrix are also present within planar laminated dolomite. Intervals with approximately 50% fenestrate microbialites are present, as are interbeds of shale, banded iron formation and diagenetic chert. Shales commonly contain calcite concretions with microbial roll-up structures (cf. Simonson & Carney, 1999).

Basinal sediments consist predominantly of fine to medium crystalline dolostones and dolomitic limestones with millimetre- to centimetre-thick laminae and nodular dolostones and dolomitic limestones (Fig. 13c). Original grain sizes have been obscured by recrystallization. Nodules consist of both dolomite and dolomitic limestone and are several centimetres in diameter and up to tens of centimetres long. Laminae extend from within the nodules to the surrounding sediment and are deformed as a result of differential compaction. In some intervals, up to half the beds contain void-filling calcite spar with fenestrate microbialite textures visible in better preserved beds (Fig. 13a). Rare breccias contain centimetre to decimetre platy clasts of uniform composition and a carbonate matrix (Fig. 13d). Commonly, breccia fabrics are fitted and transition laterally into unbrecciated layers. Interbeds of shale are common, and ferruginous chert replacement of the carbonates is common as both beds and nodules. Banded iron formation interbeds are present locally. Five to 140 cm thick interbedded tuffs are graded and current ripple cross-laminated.

Interpretation of lithofacies assemblage

The presence of fine-grained facies, paucity of cross-stratification, the presence of tuffaceous turbidites, interbeds of fenestrate microbialites, shale and iron formation, and slope soft sediment deformation strongly support a slope to basinal depositional environment for this lithofacies assemblage, as concluded by Beukes (1980, 1987). Breccias and folding show transport to the south or west and are interpreted as slope failure soft sediment deformation and debris flows. Nodular facies result from the differential cementation of sediments within the soft sediment. Later compaction affected unlithified intervening sediment. Microbial mats were present, although morphologically simpler than the shallower water fenestrate microbialite facies. Interbedding of the two lithofacies, however, suggests proximity of these two depositional environments.

In contrast to the slope to basinal environment supported by present observations, Altermann & Herbig (1991) and Hälbich *et al.* (1992) interpreted these lithofacies as peritidal based on their reported presence of a number of features, including:

1 Wave and erosional rippled mudstones – no wave or erosional ripples were observed in the Preiska facies, and the 'erosional ripples' presented by Altermann and Herbig (see Fig. 6a in Altermann & Herbig, 1991) are interpreted as elongate 'biscuit' concretions that partially merged to form semi-parallel ridges during differential modern erosion.

2 Lenticular grainstones – no distinct channels or lenticular grainstones were observed. Differential cementation and recrystallization caused some parts of beds to appear coarser grained than other parts of the beds, but distinct changes in grain size were not commonly

observed along strike, unlike in the shallower water facies.

3 Herringbone cross-stratification – Altermann & Herbig (1991) observed bidirectional cross-stratification at one site at the top of the Vryburg Formation, which was probably deposited in a shallower depositional environment than the Preiska facies (Beukes, 1987). In this study, herringbone cross-stratification in the Preiska facies was not observed.

4 Platy breccias – the platy breccias observed during field work consisted of deformed and brecciated layers (Altermann & Herbig, 1991). Here, they are interpreted as soft sediment deformation of partially lithified layers rather than current-deposited clasts.

5 'Chicken wire' structures – the quartz crystals interpreted as 'chicken wire' structure contain crystal face imprints (Altermann & Herbig, 1991) that have identical interfacial angles to dolomite rhombs projecting into the quartz crystal. This is not indicative of dissolution of a euhedral evaporite, followed by precipitation of quartz to fill the void. Instead, they are interpreted as quartz growth within sediment during diagenesis. Thus, they are not indicative of depositional conditions.

6 Polygonal cracks – polygonal patterns observed during field work did not contain cracks. Rather, the dish-shaped structures and voids filled with calcite cement are most consistent with altered fenestrate microbialites. Well-preserved cuspate microbial structures contain organic laminae that grew upwards as supports that were draped by laminate mat to form both the dish shapes and the vertical sheets interpreted as cracks by Altermann & Herbig (1991). These are here interpreted as microbial growth structures rather than as desiccation structures.

7 Oncolites/pisolites – Altermann & Herbig (1991) were uncertain of the origin of the spherical oncolites/pisolites that are up to 10 cm in diameter. These structures are probably spherical and domical chert and dolomite concretions that formed within the sediment. Depositional laminae in all spherical and domical structures observed, both chert and dolomite, project through the spheres and domes into the surrounding sediment even when diagenetic banding reflects the spherical or domical geometry (Fig. 13e). Thus, they are not diagnostic of shallow-water depositional environments.

The differences in sedimentary structures and composition between clearly identified peritidal lithofacies in the Malmani Subgroup and the Prieska lithofacies strongly support a basinal, rather than a peritidal, interpretation for the Prieska lithofacies. This interpretation is also consistent with the stratigraphic distribution of lithofacies, which shows a progressive deepening from north-east to south-west, with development of a rimmed margin between platform facies and the Prieska facies (Fig. 2; Beukes, 1987).

The proportion of calcite and aragonite that precipitated *in situ* on the seafloor in slope to basinal facies is negligible except where fenestrate microbialites are interbedded with this lithofacies assemblage. Calcite precipitated within the sediment before compaction as demonstrated by the nodular facies, and much of the brecciated sediment had to have been lithified soon after deposition. However, no calcite or aragonite encrustations precipitated in slope to basinal facies except associated with fenestrate microbialites.

Other grainstone lithofacies

Thick intervals of dolomitized grainstones, possibly containing other facies, are present in the interior of the platform, particularly in the upper half of the platform (Fig. 2). These intervals consist of centimetre- to metre-thick beds of carbonate sand containing sparsely preserved wave, interference, climbing or current ripples. Rare beds also contain either hummocky cross-stratification or trough cross-stratification. Primary grain sizes varied from silt sized to very coarse sand, and sorting is difficult to determine because of extensive recrystallization. The range in cross-stratification styles suggests deposition in environments ranging from shallow subtidal to supratidal. Grainstone-dominated intervals have not been subdivided into depositional environments where sedimentary structures are poorly preserved. When an environmental interpretation is reasonable through association with better preserved and more abundant diagnostic sedimentary structures, the grainstones are grouped into the more specific lithofacies assemblages.

In rare instances, the remnants of fibrous calcite cement textures are preserved within grainstone lithofacies as seafloor encrustations mixed with carbonate sand. These areas, however, are poorly preserved, and specific estimates of the proportion of *in situ* precipitated carbonate were deemed to be too unreliable to record accurately because of extensive recrystallization.

CARBONATE PRECIPITATION STYLES

Calcite and aragonite precipitated directly on the seafloor in all the platform facies of the Campbellrand-Malmani carbonate platform. In many open-marine environments, the proportion of carbonate that precipitated in place is at least 30% based on observed textures. Thus, the precipitation of calcite and aragonite directly on the seafloor was a major platform-building process. The importance of *in situ* precipitation varied with depositional environment, and the distribution and abundance of calcite and aragonite encrustations are interpreted as a result of variations in both the influx of clastic carbonate and local sea-water chemistry.

Sedimentation rates

The abundance of *in situ* precipitated calcite and aragonite varies inversely with the influx of detrital carbonate. The influx of sediment interrupted the growth of calcite and aragonite crystals. In many cases, aragonite pseudomorphs were buried by sediment, which stopped their growth (Sumner & Grotzinger, 2000). Similarly, areas protected from sedimentation, such as the undersides of bulbous stromatolites, were commonly coated with calcite and aragonite encrustations, whereas contemporaneous unprotected areas were not (Fig. 6a). If potential calcite and aragonite crystal growth rates were constant, variations in sedimentation rate would cause variations in the length of time a crystal could have grown; slower sedimentation rates allowed larger or more cement crystals to grow, resulting in an increased proportion of *in situ* precipitated calcite and aragonite. Occasionally, discrete depositional episodes are separated by calcite encrustations, as in the case of episodically developed shallow subtidal grainstones overlain by calcite encrustations or precipitated stromatolites (Fig. 13c and d). Also, in some deep subtidal depositional environments, the influx of sediment was low to non-existent. For example, both grainstones and micritic sediment are absent from most of the fenestrate microbialite lithofacies assemblage (Sumner, 1997a,b, 2000). The absence of sediment influx allowed thick accumulations of herringbone calcite to form. Thus, clastic carbonate influx was a critical influence on the proportion of *in situ* precipitation of carbonate with lower rates of sediment influx leading to higher proportions of precipitated carbonate.

The abundance of decimetre-thick calcite crusts and aragonite fans in shallow depositional environments requires that average sedimentation rates were low, carbonate precipitation rates were very high or a combination of both (Sumner & Grotzinger, 2000). The abundance of grainstones and breccias associated with pseudomorphed aragonite and calcite encrustations in shallow subtidal environments suggests that the encrustations grew during intervals with continuous sediment influx, and that their growth did not require long periods of time with no sediment influx (Sumner & Grotzinger, 2000). The draping of pseudomorphed aragonite fans with carbonate sediment (Figs 7 and 11a and b) suggests that crystal growth rates were very high rather than sedimentation rates being extremely slow. Although sedimentation rates may have been somewhat lower during Neoarchaean time, it is likely that crystal growth rates were substantially higher than most Proterozoic and Phanerozoic precipitation rates, possibly because of higher supersaturation of sea water with respect to calcite and aragonite (Grotzinger, 1989; Grotzinger & Kasting, 1993; Sumner & Grotzinger, 2000).

Distribution of precipitates

The abundance of aragonite and calcite encrustations varies with depositional environment as does the abundance of micrite. The distribution of aragonite as a function of depositional environment reflects a change in saturation state with depth in Neoarchaean oceans. Aragonite pseudomorphs are present only in facies deposited above wave base, suggesting that shallow water was more supersaturated with respect to aragonite, probably on account of warmer temperatures and lower CO_2 concentrations in shallow water, as in modern oceans (e.g. Plummer & Busenberg, 1982; Burton & Walter, 1987; Grammer *et al.*, 1996). Additionally, aragonite pseudomorph fans are best developed in the shallow subtidal elongate stromatolite lithofacies. The elongation of the stromatolites, as well as associated sedimentary structures and stratigraphic setting, demonstrate that this facies was deposited in open-marine environments with strong tidal circulation. Although some aragonite pseudomorph fans are present in peritidal facies, possibly associated with evaporative concentration of sea water, these fans are both smaller and less abundant than those in unrestricted facies. Open-marine, well-circulated waters seem to have promoted the precipitation of aragonite fans as a result of either

high precipitation rates or lower influxes of micrite and other clastic carbonate. In either case, the mixed layer of Neoarchaean oceans was supersaturated with respect to aragonite.

The stratigraphic distribution of *in situ* calcite precipitation covers a wider range of depositional environments. Calcite precipitated directly on the seafloor in depositional environments ranging from peritidal to below wave base. Herringbone calcite is abundant in all facies except the deepest slope and basinal facies. Radiaxial fibrous calcite is present only in peritidal to shallow subtidal depositional environments. It is not found in association with deep subtidal fenestrate microbialite lithofacies or deeper facies. The restricted distribution of radiaxial fibrous calcite relative to herringbone calcite may reflect a change in calcite precipitation with depth, with conditions more consistently promoting herringbone calcite precipitation at greater depths. Both cement textures are interpreted as fibrous Mg-calcite cements, so secondary influences such as the distribution of trace elements or organics that influence the development of specific crystal faces in Mg-calcite may control this distribution.

The transition from the deep subtidal fenestrate microbialite lithofacies to deeper water deposits shows a decrease in the abundance of herringbone calcite and an increase in the abundance of shale and siderite with some calcite precipitation within the sediment. The presence of siderite suggests an increase in Fe^{2+} concentration with depth. Reduced iron in solution slows the rate of calcite precipitation (Dromgoole & Walter, 1990a,b; Sumner *et al.*, 1999), and the transition from herringbone calcite to siderite precipitation could result from an increase in Fe^{2+} concentrations rather than a decrease in calcite saturation with depth. Iron formation accumulated in basinal facies, demonstrating high concentrations of iron in deep sea water (e.g. Ewers, 1983; Beukes & Klein, 1992; Simonson & Hassler, 1996). Thus, the change with depth to no *in situ* calcite precipitation could have resulted from inhibition of calcite precipitation by Fe^{2+} rather than a decrease in carbonate ion concentrations, although both may have played a role.

The distribution of detrital micrite in the platform also varies with depositional environment. Beds of micrite are present in shallow intertidal to supratidal depositional environments, particularly associated with the most restricted facies as demonstrated by the presence of halite casts (Fig. 5c). In contrast, micrite beds were not observed in shallow subtidal depositional environments, possibly due to more extensive agitation. Similarly, micritic cements are common in peritidal stromatolites, but most intertidal to deep subtidal stromatolites and microbialites contain fibrous calcite cements with some detrital silt- to sand-sized carbonate. In addition, lagoonal lithofacies lack micritic sediment, and most of the deep subtidal microbialite lithofacies assemblage, which was deposited in unagitated environments, contains no evidence for settling of micritic sediment (Sumner, 1997b, 2001). In rare samples that grew basinward of a rimmed platform margin, millimetre-thick laminae of silt-sized sediment (average crystal cross-section in thin section is 30 ± 10 μm) are present on the floors of voids after precipitation of variable amounts of herringbone calcite. The herringbone calcite still shows undulose extinction demonstrating that the sediment has not significantly recrystallized, and the silt size of the transported sediment is likely to be primary. In addition, the finest grained basinal carbonate samples collected show average crystal sizes of 28 ± 13 μm and, although recrystallization and coarsening of crystals cannot be entirely eliminated, micrite-sized crystals were not observed in any thin sections. Thus, crystal sizes suggest that silt- to sand-sized sediment dominated basinal environments. Although some micrite may have been deposited in slope environments, it was probably a minor component of the sediment. Small amounts of micrite could have been washed in from shallower parts of the platform, but it did not form a substantial component of deep-water sedimentation as seen in Palaeoproterozoic and younger carbonates (e.g. Knoll & Swett, 1990; Sami & James, 1994; Turner *et al.*, 1997; Sumner, 2001). This apparent paucity of micrite suggests that spontaneous precipitation of carbonate, i.e. whitings, was not common across seaward sides of the platform.

DISCUSSION

Carbonate accumulation is strongly influenced by the carbonate saturation state of sea water and the kinetics of carbonate precipitation. The distribution, abundance and mineralogy of abiotic and microbially influenced carbonate precipitates depend on the carbonate chemistry of sea water, calcium concentrations in the oceans and the global accumulation rate of carbonate sediment, among other factors. Preserved carbonates can be used to constrain ancient oceanic carbonate

chemistry. In Neoarchaean carbonates, the abundance of shallow-water aragonite pseudomorphs constrains the carbonate saturation state of Neoarchaean surface sea water to above aragonite saturation. Aragonite supersaturation requires approximately neutral to alkaline pH even with high calcium concentrations because of the rapid decrease in carbonate ion concentration with decreasing pH, especially below pH 6·35. Although broad, this pH constraint is important for reconciling atmospheric models with ocean chemistry. In the absence of atmospheric methane, modelling suggests that carbon dioxide concentrations in the Archaean atmosphere may have been up to three orders of magnitude higher than modern concentrations based on the need to maintain liquid water on earth with a fainter sun (e.g. Walker, 1983; Kasting, 1993). Lower CO_2 concentrations, including as low as modern atmospheric CO_2 levels, are possible if the Archaean atmosphere contained more than $\approx$100 p.p.m. CH_4 (Kasting *et al.*, 2001). In the absence of methane, the high predicted CO_2 concentrations could lead to slightly acidic oceans with very high concentrations of inorganic carbon (e.g. Grotzinger & Kasting, 1993). The abundance of aragonite pseudomorphs and the resulting requirement that oceanic pH was not acidic supports atmospheric models of the Neoarchaean atmosphere that contain significant concentrations of non-CO_2 greenhouse gases such as methane (Kasting *et al.*, 2001).

Calcium concentrations are also critical for determining carbonate saturation states. However, calcium fluxes to and from Neoarchaean oceans are unconstrained. Weathering rates of continental and seafloor crust are unknown for Neoarchaean time when the volume of continental crust, seafloor spreading rates, surface temperatures and atmospheric chemistry are all poorly constrained. However, high carbonate saturation states can only be maintained if global accumulation of calcium in carbonates is equal to or less than the flux of calcium into the oceans. If calcium fluxes to Neoarchaean sea water were not substantially different from those to Phanerozoic oceans, higher saturation states must have been maintained by limits on global carbonate accumulation. This could be achieved by limiting the lateral extent of carbonate accumulation resulting from limited stable continental shelf area on which to accumulate carbonates and limited accumulation of pelagic carbonates on the seafloor. Alternatively, chemical inhibitors to carbonate precipitation may have slowed the rate of carbonate precipitation in most depositional environments, much as magnesium, sulphate and organics slow the rate of abiotic and microbial carbonate precipitation in modern oceans (Berner, 1975; Busenberg & Plummer, 1985; Burton & Walter, 1988, 1990). If accumulation was restricted by limited shelf area, the Campbellrand-Malmani carbonate platform may represent one of the few areas of substantial carbonate accumulation, which allowed the rapid precipitation of calcite and aragonite locally. In contrast, if stable shelf area was abundant, carbonate accumulation must have been inhibited in many areas. In specific regions, such as those represented by the Campbellrand-Malmani carbonate platform, precipitation inhibitions could have been lower, resulting in very rapid local calcite and aragonite accumulation rates. Thus, the precipitation rate at any given location may have been very rapid if global accumulation of carbonate was either spatially or chemically limited.

Depositional textures suggest that Neoarchaean sea water was highly supersaturated with respect to aragonite, but micrite precipitation was rare in open-marine environments. Spontaneous nucleation of carbonate from modern sea water is limited by the kinetics of crystal nucleation and growth. Magnesium, sulphate and organic molecules bind to the surfaces of potential crystal nuclei, increasing their surface energy, promoting dissolution of the nuclei and restricting precipitation of micrite (Ohara & Reid, 1973; Berner, 1975; Berner *et al.*, 1978). However, marine cyanobacterial blooms can induce micrite precipitation by increasing local saturation states (e.g. Robbins & Blackwelder, 1992; Yates & Robbins, 1995). If ocean saturation states were significantly higher during Neoarchaean time, nucleation rates must also have been suppressed (Sumner & Grotzinger, 1996a; Sumner, 2001). If micrite was produced bacterially before the evolution of calcifying algae, low populations of pelagic bacteria may have limited the precipitation of micrite in the water column. However, by 2·5 Ga, cyanobacteria had evolved and diversified (e.g. Buick, 1992; Des Marais, 1994; Schopf, 1994; Summons *et al.*, 1999), suggesting that significant populations of pelagic bacteria were possible if not likely during deposition of the Campbellrand-Malmani carbonate platform. Alternatively, the chemistry of sea water could have been such that nucleation of carbonate in sea water was chemically inhibited, and conditions favoured the growth of preexisting crystals (Sumner & Grotzinger, 1996a; Sumner, 2001).

Ferrous iron and reduced manganese have been proposed as inhibitors to calcite nucleation (Sumner & Grotzinger, 1996a,b). Episodic deposition of iron formation during accumulation of the Campbellrand-Malmani carbonate platform demonstrates an abundance of iron in deep sea water (e.g. Ewers, 1983; Beukes & Klein, 1992; Simonson & Hassler, 1996). In addition, based on the abundance of aragonite pseudomorphs and neutral to alkaline pH requirements, methane may have been an important greenhouse gas implying an anoxic atmosphere (e.g. Kasting *et al.*, 2001), which is consistent with suboxic surface ocean water with low concentrations of reduced iron and manganese. If reduced iron or manganese was present in the mixed zone of the ocean, calcitic micrite precipitation may have been inhibited. However, in areas on broad platforms with limited circulation, conditions may have been more oxidizing as a result of photosynthetic production of O_2. Iron and manganese would have oxidized, and the inhibitor to micrite nucleation would have been removed, resulting in some spontaneous or microbially induced carbonate precipitation in the water column followed by deposition as micritic sediment. This model is consistent with the presence of some micrite in peritidal depositional environments of the Campbellrand-Malmani carbonate platform and its absence or paucity in deep subtidal depositional environments. However, a similar inhibitor for aragonitic micrite precipitation is also necessary; little research into the dynamics of aragonite nucleation in sea water has been reported. Thus, the distribution of iron and other potential inhibitors to carbonate precipitation, particularly aragonite precipitation, needs to be investigated further to test this model.

CONCLUSIONS

The *in situ* precipitation of calcite and aragonite on the seafloor was a major platform-building process in deposition of the Campbellrand-Malmani carbonate platform. In subtidal depositional environments, a minimum of 20% to more than 35% of the rock precipitated as encrustations on the seafloor or early marine void-filling cements. The volumetric abundance of these environments in the platform demonstrates that the dynamics of carbonate precipitation favoured growth of crystals on the seafloor as opposed to precipitation within the water column.

Aragonite pseudomorphs are abundant in open-marine, agitated depositional environments, less abundant in restricted facies and absent from sediments deposited below wave base. Calcite encrustations are volumetrically abundant in all intertidal to subtidal depositional environments except for deep slope and basinal deposits. This distribution is consistent with lower saturation states for aragonite with increasing pressure and decreasing temperature with depth in the oceans. The absence of calcite encrustations at depth may result from reduced precipitation rates due to the kinetics of calcite growth rather than a dramatic decrease in calcite saturation state.

The abundance of aragonite pseudomorphs constrains Neoarchaean sea water to neutral to alkaline pH. High saturation states may have been maintained by spatially limited carbonate accumulation or by the chemical properties of sea water. The presence of inhibitors to calcite and aragonite precipitation is suggested by the required high saturation states and the paucity of micrite in deep subtidal depositional environments.

ACKNOWLEDGEMENTS

Many thanks go to Nicolas J. Beukes, who provided extensive field support and many insightful discussions. Thanks also to Andrey Bekker and Bruce Simonson for helpful reviews. Financial support during collection of field data was provided by an NSF Graduate Fellowship and the Gretchen L. Blechschmidt Fund of GSA to D.Y.S., and by NASA grant NAGW-2795 and NSF grant EAR-9058199 to J.P.G. D.Y.S. was supported by NASA grant NAG5-10591 during compilation and writing of the manuscript.

REFERENCES

Altermann, W. (1996) Sedimentology, geochemistry and palaeogeographic implications of volcanic rocks in the upper Archaean Campbell Group, western Kaapvaal Craton, South Africa. *Precambrian Res.*, **79,** 73–100.

Altermann, W. and **Herbig, H.C.** (1991) Tidal flat deposits of the Lower Proterozoic Campbell Group along the southwestern margin of the Kaapvaal Craton, Northern Cape Province, South Africa. *J. Afr. Earth Sci.*, **13,** 415–435.

Altermann, W. and **Nelson, D.R.** (1998) Sedimentation rates, basin analysis and regional correlations of three Neoarchaean and Paleoproterozoic sub-basins of the Kaapvaal Craton as inferred from precise U-Pb zircon ages from volcaniclastic sediments. *Sed. Geol.*, **120,** 225–256.

Armstrong, R.A., Compston, W., Retief, E.A., Williams, I.S. and **Welke, H.J.** (1991) Zircon ion microprobe studies bearing on the age and evolution of the Witwatersrand triad. *Precambrian Res.*, **53,** 243–266.

Barton, E.S., Altermann, W., Williams, I.S. and **Smith, C.B.** (1994) U-Pb zircon age for a tuff in the Campbell Group, Griqualand West Sequence, South Africa: implication for Early Proterozoic rock accumulation rates. *Geology*, **22,** 343–346.

Bekker, A. and **Eriksson, K.A.** (2003) Paleoproterozoic drowned carbonate platform on the southeastern margin of the Wyoming Craton: a record of the Kenorland breakup. *Precambrian Res.*, **120,** 327–364.

Berner, R.A. (1975) The role of magnesium in the crystal growth of calcite and aragonite from seawater. *Geochim. Cosmochim. Acta*, **39,** 489–504.

Berner, R.A., Westrich, J.T., Graber, R., Smith, J. and **Martens, C.S.** (1978) Inhibition of aragonite precipitation from supersaturated seawater; a laboratory and field study. *Am. J. Sci.*, **278,** 816–837.

Bertrand-Sarfati, J. and **Eriksson, K.A.** (1977) Columnar stromatolites from the Early Proterozoic Schmidtsdrift Formation, northern Cape Province, South Africa – Part 1: systematic and diagnostic features. *Palaeontol. Africana*, **20,** 1–26.

Beukes, N.J. (1977) Transition from siliciclastic to carbonate sedimentation near the base of the Transvaal Supergroup, northern Cape Province, South Africa. *Sed. Geol.*, **18,** 201–221.

Beukes, N.J. (1980) Stratigrafie en litofasies van die Campbellrand-subgroep van die Proterofitiese Ghaap-groep, noord-Kaapland. *Trans. Geol. Soc. S. Afr.*, **83,** 141–170.

Beukes, N.J. (1983) Ooids and oolites of the Proterophytic Boomplaas Formation, Transvaal Supergroup, Griqualand West, South Africa. In: *Coated Grains* (Ed. T.M. Peryt), pp. 199–214. Springer-Verlag, Berlin.

Beukes, N.J. (1987) Facies relations, depositional environments and diagenesis in a major early Proterozoic stromatolitic carbonate platform to basinal sequence, Campbellrand Subgroup, Transvaal Supergroup, southern Africa. *Sed. Geol.*, **54,** 1–46.

Beukes, N.J. and **Klein, C.** (1992) Models for iron-formation deposition. In: *The Proterozoic Biosphere* (Eds J.W. Schopf and C. Klein), pp. 147–151. Cambridge University Press, Cambridge.

Beukes, N.J. and **Smit, C.A.** (1987) New evidence for thrusting in Griqualand West, South Africa: Implications for stratigraphy and the age of red beds. *S. Afr. J. Geol.*, **90,** 378–394.

Buick, R. (1992) The antiquity of oxygenic photosynthesis: evidence from stromatolites in sulphate-deficient Archean lakes. *Science*, **255,** 74–77.

Burton, E.A. and **Walter, L.M.** (1987) Relative precipitation rates of aragonite and Mg calcite from seawater: temperature or carbonate ion control? *Geology*, **15,** 111–114.

Burton, E.A. and **Walter, L.M.** (1988) Experimental investigation of Mg/Ca and sulfate as controls on temporal variations in mineralogy of marine carbonates. *Geol. Soc. Am., Abstracts with Programs*, **20,** 219.

Burton, E.A. and **Walter, L.M.** (1990) The role of pH in phosphate inhibition of calcite and aragonite precipitation rates in seawater. *Geochim. Cosmochim. Acta*, **54,** 797–808.

Busenberg, E. and **Plummer, L.N.** (1985) Kinetic and thermodynamic factors controlling the distribution of $SO42^{-}$ and Na^{+} in calcites and aragonites. *Geochim. Cosmochim. Acta*, **49,** 713–725.

Button, A. (1973) The stratigraphic history of the Malmani dolomite in the eastern and north-eastern Transvaal. *Trans. Geol. Soc. S. Afr.*, **76,** 229–247.

Clay, A.N. (1986) The stratigraphy of the Malmani Dolomite Subgroup in the Carletonville area, Transvaal: genetic implications for lead-zinc mineralization. In: *Mineral Deposits of Southern Africa* (Eds C.R. Anhaeusser and S. Maske), pp. 853–860. Geological Society of South Africa, Johannesburg.

Clendenin, C.W. (1989) *Tectonic influence on the evolution of the Early Proterozoic Transvaal Sea, Southern Africa*. Doctoral Thesis, University of the Witwatersrand, Johannesburg.

Clendenin, C.W., Henry, G. and **Charlesworth, E.G.** (1991) Characteristics of and influences on the Black Reef depositional sequence in the eastern Transvaal. *S. Afr. J. Geol.*, **94,** 321–327.

Des Marais, D.J. (1994) The Archean atmosphere; its composition and fate. In: *Archean Crustal Evolution*, (Ed. K.C. Condie), *Developments in Precambrian Geology*, **11,** pp. 505–523. Elsevier, Amsterdam.

Dromgoole, E.L. and **Walter, L.M.** (1990a) Inhibition of calcite growth rates by $Mn2^{+}$ in $CaCl_2$ solutions at 10, 25, and 50°C. *Geochim. Cosmochim. Acta*, **54,** 2991–3000.

Dromgoole, E.L. and **Walter, L.M.** (1990b) Iron and manganese incorporation into calcite: Effects of growth kinetics, temperature and solution chemistry. *Chem. Geol.*, **81,** 311–336.

Duane, M.J., Kruger, F.J., Roberts, P.J. and **Smith, G.B.** (1991) Pb and Sr isotope and origin of Proterozoic base metal (fluorite) and gold deposits, Transvaal Sequence, South Africa. *Econ. Geol.*, **86,** 1491–1505.

Eriksson, K.A. (1977) Tidal flat and subtidal sedimentation in the 2250 MY Malmani dolomite, Transvaal, South Africa. *Sed. Geol.*, **18,** 223–244.

Eriksson, K.A. and **Truswell, J.F.** (1974) Stratotypes from the Malmani Subgroup northwest of Johannesburg, South Africa. *Trans. Geol. Soc. S. Afr.*, **77,** 211–222.

Eriksson, K.A., McCarthy, T.S. and **Truswell, J.F.** (1975) Limestone formation and dolomitization in a lower Proterozoic succession from South Africa. *J. Sed. Petrol.*, **45,** 604–614.

Eriksson, K.A., Truswell, J.F. and **Button, A.** (1976) Palaeoenvironmental and geochemical models from an early Proterozoic carbonate succession in South Africa. In: *Stromatolites* (Ed. M.R. Walter), pp. 635–643. Elsevier, New York.

Ewers, W.E. (1983) Chemical factors in the deposition and diagenesis of banded iron-formation. In: *Iron-Formation Facts and Problems* (Eds A.F. Trendall and R.C. Morris), pp. 491–512. Elsevier, Amsterdam.

Grammer, G.M., McNeill, D.F. and **Crescini, C.M.** (1996) Quantifying rates of syndepositional marine cementation across a carbonate platform and margin, Bahamas. *Geol. Soc. Am., Abstracts with Programs*, **28,** 337.

Grey, K. and **Thorne, A.M.** (1985) Biostratigraphic significance of stromatolites in upward shallowing sequences of the early Proterozoic Duck Creek Dolomite, Western Australia. *Precambrian Res.*, **29,** 183–206.

Grotzinger, J.P. (1986) Cyclicity and paleoenvironmental dynamics, Rocknest platform, northwest Canada. *Geol. Soc. Am. Bull.*, **97,** 1208–1231.

Grotzinger, J.P. (1989) Facies and evolution of Precambrian carbonate depositional systems: Emergence of the modern platform archetype. In: *Controls on Carbonate Platform and*

Basin Development (Eds P.D. Crevello, J.L. Wilson, J.F. Sarg and J.F. Read), pp. 79–106. SEPM, Tulsa.

Grotzinger, J.P. (1990) Geochemical model for Proterozoic stromatolite decline. *Am. J. Sci.*, **290-A,** 80–103.

Grotzinger, J.P. and **Kasting, J.F.** (1993) New constraints on Precambrian ocean composition. *J. Geol.*, **101,** 235–243.

Grotzinger, J.P. and **Knoll, A.H.** (1995) Anomalous carbonate precipitates: is the Precambrian the key to the Permian? *Palaios*, **10,** 578–596.

Grotzinger, J.P. and **Rothman, D.H.** (1996) An abiotic model for stromatolite morphogenesis. *Nature*, **383,** 423–425.

Hälbich, I.W., Lamprecht, D., Altermann, W. and **Horstmann, U.E.** (1992) A carbonate-banded iron formation transition in the Early Protorezoicum of South Africa. *J. Afr. Earth Sci.*, **15,** 217–236.

Hardie, L.A. (1996) Secular variation in seawater chemistry: an explanation for the coupled secular variation in the mineralogies of marine limestones and potash evaporites over the past 600 my. *Geology*, **24,** 279–283.

Hofmann, A., Dirks, P.H.G.M. and **Jelsma, H.A.** (2004) Shallowing-upward carbonate cycles in the Belingwe Greenstone Belt, Zimbabwe: a record of Archean sea-level oscillations. *J. Sed. Res.*, **74,** 64–81.

Hofmann, H.J. (1971) Precambrian fossils, pseudofossils, and problematica in Canada. *Geol. Surv. Can. Bull.*, **189,** 1–146.

Hofmann, H.J. and **Masson, M.** (1994) Archean stromatolites from Abitibi greenstone belt, Quebec, Canada. *Geol. Soc. Am. Bull.*, **106,** 424–429.

Hofmann, H.J., Thurston, P.C. and **Wallace, H.** (1985) Archean Stromatolites from Uchi greenstone belt, Northwestern Ontario. In: *Evolution of Archean Supracrustal Sequences* (Eds L.D. Ayres, P.C. Thurston, K.D. Card and W. Weber), *Geol. Assoc. Can. Spec. Paper*, **28,** 1125–1132.

Hoffman, P.F. (1969) Proterozoic paleocurrents and depositional history of the East Arm fold belt, Great Slave Lake, Northwest Territories. *Can. J. Earth Sci.*, **6,** 441–462.

Hoffman, P.F. (1988) Pethei reef complex (1.9 Ga), Great Slave Lake, NWT. In: *Reefs, Canada and Adjacent Areas* (Eds H.H.J. Geldsetzer, N.P. James and G.E. Tebbutt), pp. 38–48, Canadian Society of Petroleum Geologists, Calgary.

James, N.P., Narbonne, G.M. and **Kyser, T.K.** (2001) Late Neoproterozoic cap carbonates: Mackenzie Mountains, northwestern Canada: precipitation and global glacial meltdown. *Can. J. Earth Sci.*, **38,** 1229–1262.

Kah, L.C. and **Knoll, A.H.** (1996) Microbenthic distribution in Proterozoic tidal flats: environmental and taphonomic considerations. *Geology*, **24,** 79–82.

Kasting, J.F. (1993) Earth's early atmosphere. Special section; evolution of atmospheres. *Science*, **259,** 920–926.

Kasting, J.A., Pavlov, A.A. and **Siefert, J.L.** (2001) A coupled ecosystem-climate model for predicting the methane concentrations in the Archean atmosphere. *Origins Life Evol. Biosph.*, **31,** 271–285.

Knoll, A.H. and **Swett, K.** (1990) Carbonate deposition during the later Proterozoic Era: an example from Spitsbergen. *Am. J. Sci.*, **290-A,** 104–132.

Kusky, T.M. and **Hudleston, P.J.** (1999) Growth and demise of an Archean carbonate platform, Steep Rock Lake, Ontario, Canada. *Can. J. Earth Sci.*, **36,** 565–584.

Lowenstein, T.K. and **Hardie, L.A.** (1985) Criteria for the recognition of salt-pan evaporites. *Sedimentology*, **32,** 627–644.

Martini, J.E.J. (1976) The fluorite deposits in the Dolomite Series of the Marico District, Transvaal, South Africa. *Econ. Geol.*, **71,** 625–635.

Miyano, T. and **Beukes, N.J.** (1984) Phase relations of stilpnomelane, ferri-annite, and riebeckite in very low-grade metamorphosed iron-formations. *Trans. Geol. Soc. S. Afr.*, **87,** 111–124.

Nogueira, A.C.R., Riccomini, C., Sial, A.N., Moura, C.A.V. and **Fairchild, T.R.** (2003) Soft-sediment deformation at the base of the Neoproterozoic Puga cap carbonate (southwestern Amazon craton, Brazil): confirmation of rapid icehouse to greenhouse transition in snowball Earth. *Geology*, **31,** 613–616.

Ohara, M. and **Reid, R.C.** (1973) *Modeling Crystal Growth Rates from Solution*. Prentice Hall, Englewood Cliffs, NJ, 272 pp.

Opdyke, B.N. and **Wilkinson, B.H.** (1993) Carbonate mineral saturation state and cratonic limestone accumulation. *Am. J. Sci.*, **293,** 217–234.

Pelechaty, S.M. and **Grotzinger, J.P.** (1988) Stromatolite bioherms of a 1.9 Ga foreland basin carbonate ramp, Beechey Formation, Kilohigok Basin, Northwest Territories. In: *Reefs, Canada and Adjacent Areas* (Eds H.H.J. Geldsetzer, N.P. James and G.E. Tebbutt), pp. 93–104. Canadian Society of Petroleum Geologists, Calgary.

Plummer, L.N. and **Busenberg, E.** (1982) The solubilities of calcite, aragonite and vaterite in CO_2-H_2O solutions between 0 and 90°C, and an evaluation of the aqueous model for the system $CaCO_3$-CO_2-H_2O. *Geochim. Cosmochim. Acta*, **46,** 1011–1040.

Robbins, L.L. and **Blackwelder, P.L.** (1992) Biochemical and ultrastructural evidence for the origin of whitings; a biologically induced calcium carbonate precipitation mechanism. *Geology*, **20,** 464–468.

Sami, T.T. and **James, N.P.** (1994) Peritidal carbonate platform growth and cyclicity in an early Proterozoic foreland basin, Upper Pethei Group, northwest Canada. *J. Sed. Res.*, **B64,** 111–131.

Sandberg, P.A. (1985) Nonskeletal aragonite and pCO_2 in the Phanerozoic and Proterozoic. In: *The Carbon Cycle and Atmospheric CO2: Natural Variations Archean to Present* (Eds E.T. Sundquist and W.S. Broecker), pp. 585–594. American Geophysical Union, Washington.

Schmitz, M.D. and **Bowring, S.A.** (2003a) Constraints on the thermal evolution of continental lithosphere from U-Pb accessory mineral thermochronometry of lower crustal xenoliths, southern Africa. *Contrib. Mineral. Petrol.*, **144,** 592–618.

Schmitz, M.D. and **Bowring, S.A.** (2003b) Ultrahigh-temperature metamorphism in the lower crust during Neoarchean Ventersdorp rifting and magmatism, Kaapvaal Craton, southern Africa. *Geol. Soc. Am. Bull.*, **115,** 533–548.

Schopf, J.W. (1994) The oldest known records of life: Early Archean stromatolites, microfossils, and organic matter. In: *Early Life on Earth* (Ed. S. Bengtson), pp. 193–206. Columbia University Press, New York.

Simonson, B.M. and **Carney, K.E.** (1999) Roll-up structures: evidence of *in situ* microbial mats in late archean deep shelf environments. *Palaios*, **14,** 12–24.

Simonson, B.M. and **Hassler, S.W.** (1996) Was the deposition of large Precambrian iron formations linked to major marine transgressions? *J. Geol.*, **104,** 665–676.

Simonson, B.M., Schubel, K.A. and **Hassler, S.W.** (1993) Carbonate sedimentology of the early Precambrian Hamersley Group of Western Australia. *Precambrian Res.*, **60,** 287–335.

Stowe, C.W. (1986) Synthesis and interpretation of structures along the north–eastern boundary of the Namaqua tectonic

province, South Africa. *Trans. Geol. Soc. S. Afr.*, **89,** 185–198.

Summons, R.E., Jahnke, L.L., Hope, J.M. and **Logan, G.A.** (1999) 2-Methylhopanoids as biomarkers for cyanobacterial oxygenic photosynthesis. *Nature*, **400,** 554–557.

Sumner, D.Y. (1995) Facies, paleogeography, and carbonate precipitation on the Archean (2520 Ma) Campbellrand-Malmani Carbonate Platform, Transvaal Supergroup, South Africa. Doctoral Thesis, Massachusetts Institute of Technology, Cambridge, MA, 514 pp.

Sumner, D.Y. (1997a) Carbonate precipitation and oxygen stratification in late Archean seawater as deduced from facies and stratigraphy of the Gamohaan and Frisco formations, Transvaal Supergroup, South Africa. *Am. J. Sci.*, **297,** 455–487.

Sumner, D.Y. (1997b) Late Archean calcite–microbe interactions: two morphologically distinct microbial communities that affected calcite nucleation differently. *Palaios*, **12,** 300–316.

Sumner, D.Y. (2000) Microbial versus environmental influences on the morphology of Late Archean fenestrate microbialites. In: *Microbial Sediments* (Eds R.E. Riding and S.M. Awramik), pp. 307–314. Springer Verlag, Berlin.

Sumner, D.Y. (2001) Decimeter-thick encrustations of calcite and aragonite on the sea floor and implications for Neoarchean and Neoproterozoic ocean chemistry. In: *Precambrian Sedimentary Environments: a Modern Approach to Ancient Depositional Systems* (Eds W. Altermann and P.L. Corcoran), *IAS Spec. Publ.*, **33,** 107–120.

Sumner, D.Y. and **Bowring, S.A.** (1996) U-Pb geochronologic constraints on deposition of the Campbellrand Subgroup, Transvaal Supergroup, South Africa. *Precambrian Res.*, **78,** 25–35.

Sumner, D.Y. and **Grotzinger, J.P.** (1993) Numerical modeling of ooid size and the problem of Neoproterozoic giant ooids. *J. Sed. Petrol.*, **63,** 974–982.

Sumner, D.Y. and **Grotzinger, J.P.** (1996a) Were kinetics of Archean calcium carbonate precipitation related to oxygen concentration? *Geology*, **24,** 119–122.

Sumner, D.Y. and **Grotzinger, J.P.** (1996b) Herringbone calcite: petrography and environmental significance. *J. Sed. Res.*, **66,** 419–429.

Sumner, D.Y. and **Grotzinger, J.P.** (2000) Late Archean aragonite precipitation: petrography, facies associations, and environmental significance. In: *Carbonate Sedimentation and Diagenesis in the Evolving Precambrian World* (Eds J.P. Grotzinger and N.P. James), *SEPM Spec. Publ.*, **33,** 107–120.

Sumner, D.Y., Fenger, T. and **Tourre, S.A.** (1999) Effects of reduced iron on calcite crystal morphology and implications for tracing paleoenvironmental chemistry. AGU Fall Meeting, San Francisco. http://www.agu.org/meetings/waisfm99.html.

Tinker, J., de Wit, M. and **Grotzinger, J.** (2002) Seismic stratigraphic constraints on Neoarchean-Paleoproterozoic evolution of the western margin of the Kaapvaal craton, South Africa. *S. Afr. J. Geol.*, **105,** 107–134.

Truswell, J.F. and **Eriksson, K.A.** (1972) The morphology of stromatolites from the Transvaal Dolomite north-west of Johannesburg, South Africa. *Trans. Geol. Soc. S. Afr.*, **75,** 99–110.

Truswell, J.F. and **Eriksson, K.A.** (1973) Stromatolitic associations and their palaeo-environmental significance: a reappraisal of a lower Proterozoic locality from the northern Cape Province, South Africa. *Sed. Geol.*, **10,** 1–23.

Turner, E.C., James, N.P. and **Narbonne, G.M.** (1997) Growth dynamics of Neoproterozoic calcimicrobial reefs, Mackenzie Mountains, northwestern Canada. *J. Sed. Res.*, **67,** 437–450.

Tyler, N. (1979) The stratigraphy of the early-Proterozoic Buffalo Springs Group in the Thabazimbi area, west-central Transvaal. *Trans. Geol. Soc. S. Afr.*, **82,** 215–226.

Walker, J.C.G. (1983) Possible limits on the composition of the Archean ocean. *Nature*, **302,** 518–520.

Walraven, F. and **Martini, J.** (1995) Zircon Pb-evaporation age determinations of the Oak Tree Formation, Chuniespoort Group, Transvaal Sequence: implications for Transvaal-Griqualand West basin correlations. *S. Afr. J. Geol.*, **98,** 58–67.

Wilkinson, B.H. and **Given, R.K.** (1986) Secular variation in abiotic marine carbonates: Constraints on Phanerozoic atmospheric carbon dioxide contents and oceanic Mg/Ca ratios. *J. Geol.*, **94,** 321–333.

Wilks, M.E. (1986) *The geology of the Steep Rock Group, NW Ontario: a major Archean unconformity and Archean stromatolites*. MSc Thesis, University of Saskatchewan, 206 pp.

Yates, K.K. and **Robbins, L.L.** (1995) Experimental evidence for a $CaCO_3$ precipitation mechanism for marine *Synechocystis. Bull. Inst. Océanogr. Monaco*, **14.2,** 51–59.

Young, R.B. (1932) The occurrence of stromatolitic or algal limestones in the Campbell Rand Series, Griqualand West. *Trans. Geol. Soc. S. Afr.*, **35,** 29–36.

Manuscript received 20 May 2003; revision accepted 18 November 2003.